UNCLASSIFIED

AD NUMBER
ADB022802
LIMITATION CHANGES

TO:

Approved for public release; distribution is unlimited.

FROM:

Distribution authorized to U.S. Gov't. agencies only; Administrative/Operational Use; OCT 1973. Other requests shall be referred to Naval Air Propulsion Test Center, Trenton, NJ.

AUTHORITY

USNAPTC ltr 26 Apr 1978

THIS PAGE IS UNCLASSIFIED

FR-5936

FAN/RAM DUCT PROGRAM

PHASE I FINAL REPORT

OCTOBER 1973

D. E. Booz, A. Levesque, and E. B. Thayer
Pratt & Whitney Aircraft
Division of United Aircraft Corporation
Florida Research and Development Center

DDC

NOV 11 1977

Contract N00140-73-C-0003

Naval Air Propulsion Test Center
Trenton, N. J. 08628
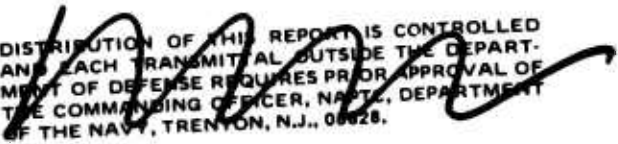
2

FAN/RAM DUCT PROGRAM

PHASE I FINAL REPORT

OCTOBER 1973

D. E. Booz, A. Levesque, and E. B. Thayer
Pratt & Whitney Aircraft
Division of United Aircraft Corporation
Florida Research and Development Center

Contract N00140-73-C-0003

Naval Air Propulsion Test Center
Trenton, N. J. 08628

CONTENTS

SECTION I

INTRODUCTION AND SUMMARY

The turbofan-ramjet combination cycle engine is a new concept in high-Mach propulsion systems that combines the subsonic specific fuel consumption advantages of a turbofan and the acceleration capability of an augmented turbofan with the ramjet needed for flight at Mach 4.5. Mission studies have indicated that this engine cycle is the most attractive cycle for the advanced high-Mach interceptor aircraft being studied for the 1980's, particularly for mission profiles that include loiter. One area of concern is the operational characteristics and control during the transition from augmented turbofan to ramjet. A large number of variables (fuel flows, shutoff doors, nozzle areas, etc.) must be programed and scheduled correctly in order to achieve a smooth, stable transition without aircraft inlet unstarts or fan stability problems. A three-phase program addressed to this area of concern was therefore planned to provide the information needed to substantiate this cycle concept. The planned program will generate a dynamic simulation of the engine system and an aerodynamic test rig design in the first phase, and culminate in an integrated test of the engine aerodynamic rig with a model aircraft inlet in the third phase.

The Phase I program reported herein is the initial 12-month effort. It started with an analysis of the aerodynamics of the combination fan duct/ram duct used in the P&WA™ STFR J368 turbofan-ramjet study engine. This was followed by the design of an aerodynamic test rig simulating the fan/ram duct configuration, including a model fan. The rig will be tested in Phase II to provide aerodynamic data (loss coefficients, flow profiles, etc.) at various steady-state points during the transition in support of the aerodynamic analysis of the fan/ram duct conducted in Phase I.

The digital dynamic engine simulation computer program was formulated and checked out during Phase I. The checkout of the program was carried through transition test cases to validate the simulation. However, it should be noted that these test cases do not represent designed or optimized transitions; they only illustrate that the computer program is operational. The computer program will then be used for transition control studies in Phase II to define the control system and logic required for engine operation and transition.

Phase III is currently envisioned as tests of the fan/ram duct rig combined with a model aircraft inlet, with the objective of demonstrating a controlled, stable transition at high Mach in a wind tunnel.

This report presents the results of the Phase I studies.

1

SECTION II

ENGINE DESCRIPTION

The P&WA STFRJ36s turbofan-ramjet study engine, shown in figure 1, was designed to provide high performance for advanced interceptors from subsonic speeds up to Mach 4.5. The design consists of a turbofan core engine housed in a wraparound duct that is common to both fan and ram airstreams, which is termed the fan/ram duct.

Below a Mach number of approximately 3.0, the fan/ram duct is pressurized by fan flow, and thrust augmentation is achieved from the fan duct heater. The ram airstream is shut off during core engine and fan duct burner operation by closing a set of vanes in the forward end of the ram duct. Above Mach 3.0, the core engine is shut off by closing a similar set of vanes just aft of the fan and by closing the core engine exhaust nozzle. In this mode, the ram duct operates as a normal subsonic combustion ramjet. Both the fan and ram duct burners are swirl combustors chosen for this engine for their high heat release and short length characteristics.

The core engine is a two-spool turbofan with an overall design pressure ratio of 25:1 and a bypass ratio of 3:1. The low rotor consists of a two-stage, 2.5:1 pressure ratio fan driven by a three-stage turbine. The high rotor has an axial-centrifugal compressor with single-stage turbine. The primary burner is also a swirl combustor, and provides near-stoichiometric turbine inlet temperatures.

Although the high pressure turbine has high work requirements, a single-stage design is sufficient with the high turbine inlet temperature available. The air necessary to provide turbine cooling is bled from compressor discharge. A three-stage low pressure turbine was chosen to satisfy the work requirements associated with high bypass ratio and high Mach number.

The bearings designed for the high speed rotor are based on DN values of 3×10^6, the maximum value predicted for growth engines in the 1980's. The bearings designed for the low speed (fan) rotor are based on the maximum size that can be incorporated within the inside diameter of the high speed rotor shaft. The engine design also incorporates an advanced accessory drive concept that permits the use of a lightweight, unitized, and remote-mounted engine control and accessory packages to reduce engine frontal area for high Mach number operation.

The nozzles used on this engine consist of an expanding-plug core engine nozzle, and an annular convergent-divergent duct nozzle. The duct nozzle design includes actuated convergent flaps with mechanically damped, aerodynamically actuated (pressure balanced) divergent flaps. The core engine plug expands to close off the core airflow, and in so doing forms an extension to the inner wall of the duct plug, providing an efficient annular C-D nozzle for the duct flow.

RAMJET INLET

FAN INLET

FAN/RAM DUCT

TURBOFAN CORE ENGINE

SHUTOFF VANES
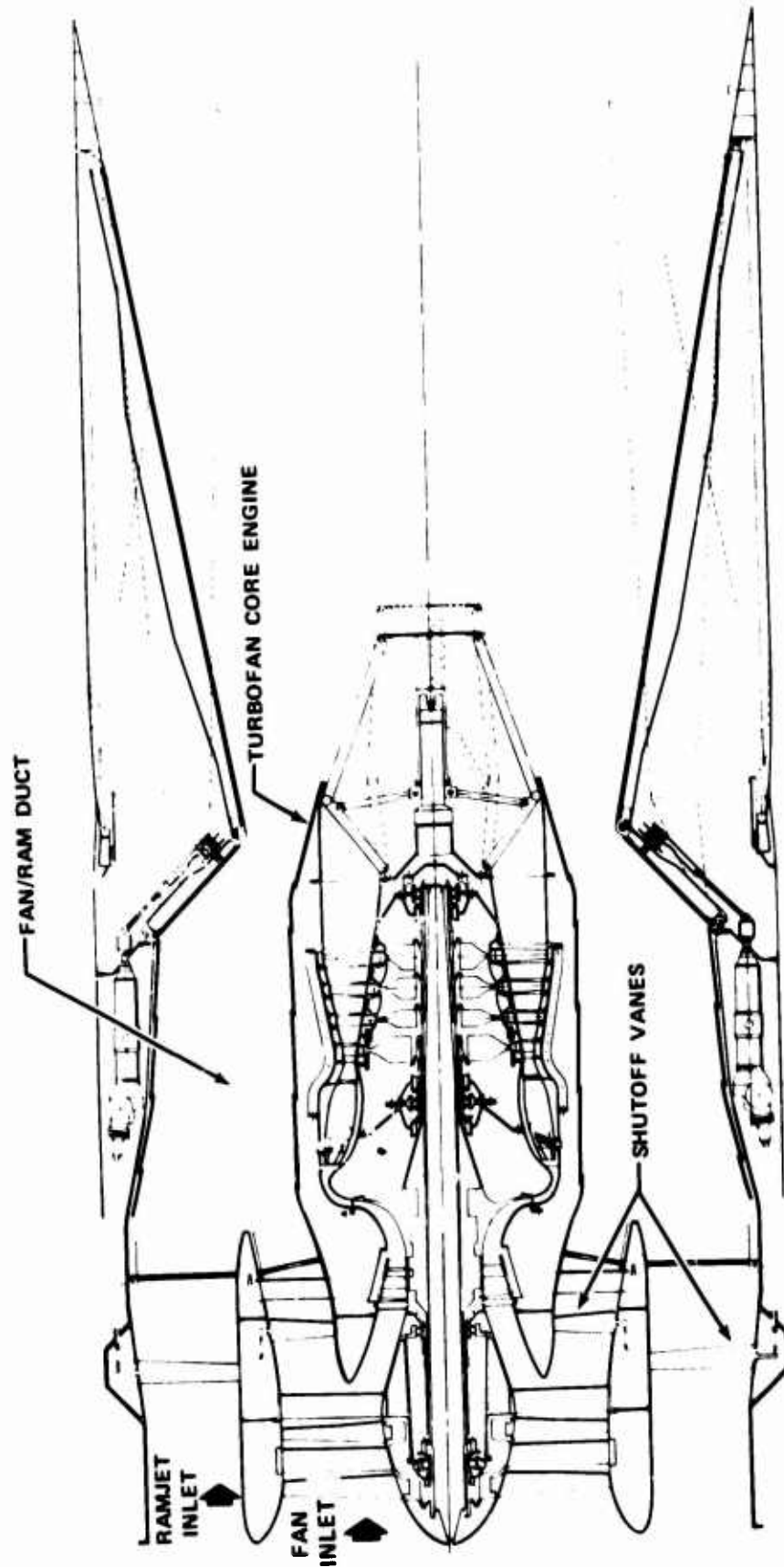
FD 73657

Figure 1. STFRJ368 Turbofan–Ramjet Engine

3

SECTION III

AERODYNAMIC DESIGN STUDY

A. GENERAL

The purpose of this study was to perform an aerodynamic design analysis of the fan and ram ducts of the STFRJ368 engine. The results are a preliminary design layout of the fan/ram duct flowpath, including the combustors, and an estimate of the system pressure losses. These results were subsequently used to design a scale model test rig of the fan/ram duct configuration, described in Section IV of this report. The estimated pressure losses were incorporated into the engine dynamic simulation, described in Section V, as a best-estimate until test data are generated in rig tests planned under Phase II of the program.

The first step in the aerodynamic design was to select the basic engine design points, which are as follows:

Turbofan design point: 250 lb/sec airflow at SLS
Ramjet design point: 155 lb/sec airflow at Mach 3.0, 75,000 ft
Turbofan operating range: SLTO to Mach 3.5
Ramjet operating range: Mach 2.5 to 4.5
Turbofan to ramjet transition range: Mach 2.5 to 3.5

With these engine design points and operating ranges chosen, internal flow conditions were then calculated with the engine cycle deck to provide the pressures, temperatures, etc., needed to size the fan/ram duct flowpath, to design the combustion system, to analyze the fan/ram duct flow field, and to estimate the system pressure losses. Each of these areas is discussed below in a separate section. To provide consistent locations for critical points in the flowpath, numerical engine stations were designated as shown in figure 2. These engine station designations comply with SAE ARP 1257: <u>Aerospace Recommended Practice -- Gas Turbine Engine Transient Performance Presentation for Digital Computer Programs</u>, June 1972.

B. FLOWPATH DEFINITION

The preliminary design layout of the fan and ram duct flowpaths of the STFRJ368 engine is shown in figure 3. Definition of the flowpath included sizing the flow areas at critical points and selection of the flowpath wall contours to give low pressure losses. An equivalent conical diffuser angle of 11.4 deg was selected for the fan duct diffuser and 8.0 deg for the ram duct diffuser, where length was not a prime consideration. The core engine support struts, which cross both the fan and ram ducts, were sized based on the most severe stress condition, which was assumed to occur at 3.5 rad/sec yaw with 1 g maneuver load. Eight struts, each with a 10.3-in. chord and a 12% thickness/chord ratio, were determined to be required.

4
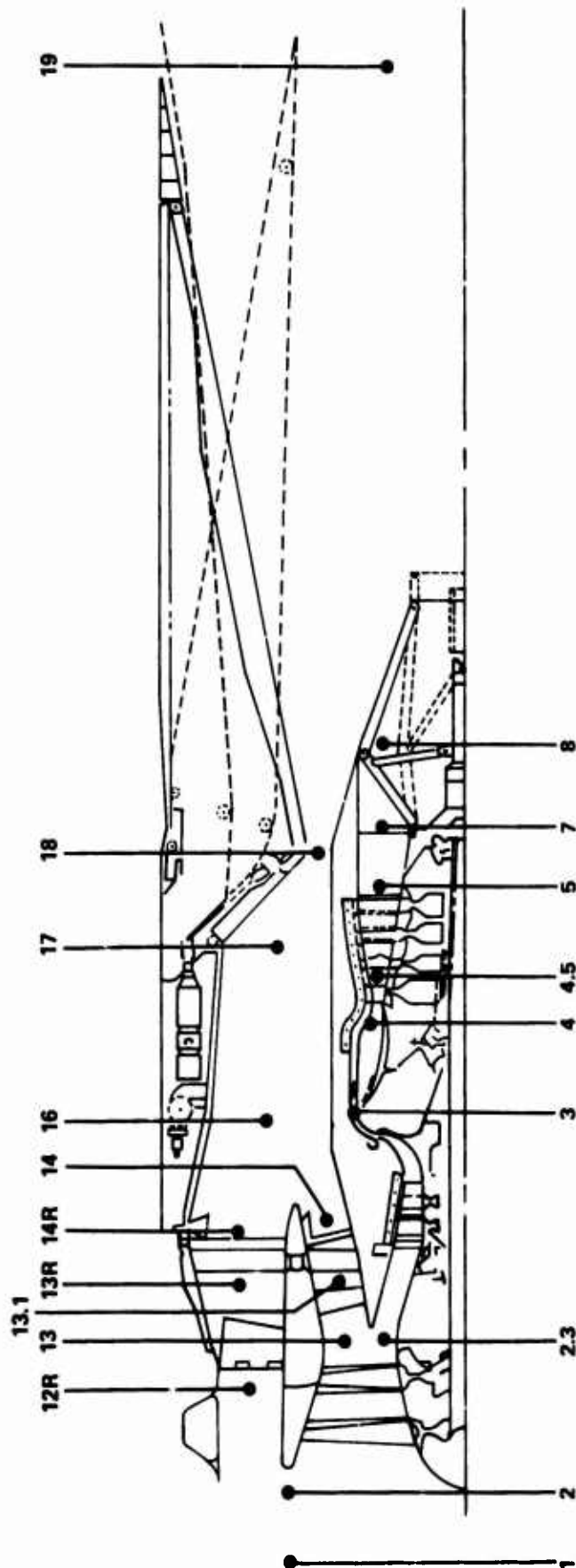
1 . INLET-ENGINE INTERFACE
2 . ENGINE FACE
2.3 . HIGH PRESSURE COMPRESSOR INLET
3 . MAIN BURNER INLET
4 . MAIN BURNER EXIT
4.5 . LOW PRESSURE TURBINE INLET
5 . LOW PRESSURE TURBINE EXIT
7 . CORE ENGINE NOZZLE INLET
8 . CORE ENGINE NOZZLE THROAT
13 . FAN DUCT INLET

13.1 . FAN DUCT BURNER INLET
14 . FAN DUCT BURNER EXIT
12R . RAMJET INLET
13R . RAMJET BURNER INLET
14R . RAMJET BURNER EXIT
16 . DUCT INLET
17 . DUCT NOZZLE INLET
18 . DUCT NOZZLE THROAT
19 . DUCT NOZZLE EXIT

FD 73658

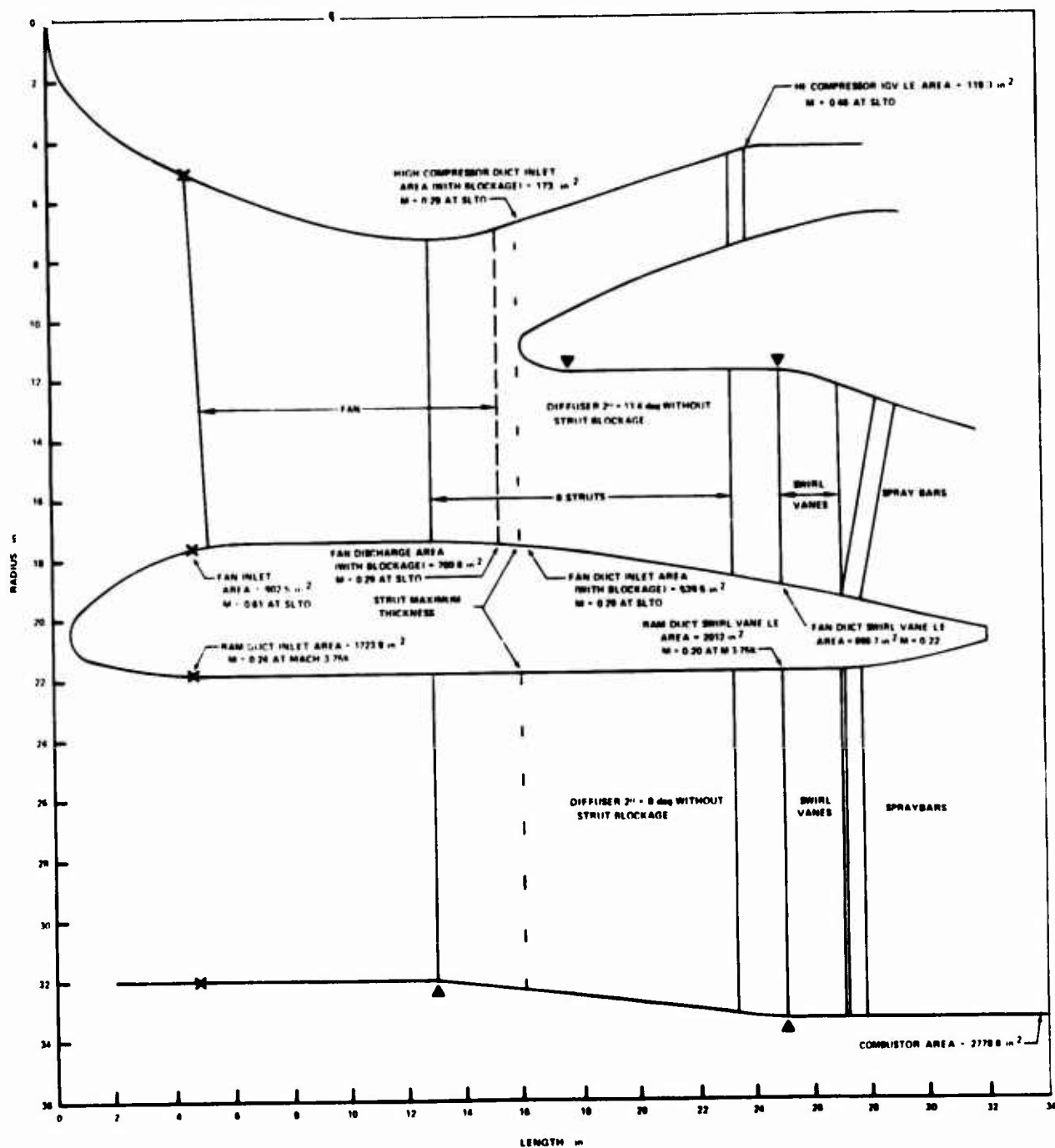Figure 2. STFRJ368 Turbofan-Ramjet Station Designation

5

Figure 3. STFRJ368 Preliminary Fan/Ram Duct Flow Path

FD 73659

Split-strut shutoff doors were initially chosen for both the fan and ram ducts because of the simpler actuation system required compared to other types considered. This type of door consists of two sheet metal panels that fit against the skin of the support struts when retracted. They are hinged at the leading edge of the struts, and, when extended, block half of the passage between two adjacent struts. The panel on the next strut blocks the other half of the flow passage. These types of doors, however, require that the ID of the flow passage be flat in order to completely close the passage. Thus, the OD of the fan/ram duct flow splitter, and the OD of the core engine flow splitter, would have had to be octagonal to provide the necessary flats between the struts.

After a design review, it was decided to change the door design to eliminate the disadvantages of the octagonal-shaped inner walls of the fan and ram ducts, and to reduce the large actuation forces associated with the split-strut type doors. The final door design, a set of rotating vanes in both fan and ram ducts, is shown in figure 4. In the fan duct, 48 zero-camber, rotating vanes were located upstream of the fixed, cambered, swirl vanes, whereas in the ram duct, the shutoff door and swirl vane functions were combined in a set of 112 cambered rotating vanes at an axial location near mid chord of the eight support struts. By using a relatively large number of rotating vanes in each duct, round cases can be used for the duct inner walls without excessive leakage. The advantages of round-over octagonal cases are elimination of circumferential velocity distortions, smoother flow splitter contours (especially the core flow-fan flow splitter), and better structural characteristics. The disadvantages of rotating vanes are slightly higher duct blockages in the open position and a greater number of parts required.

C. COMBUSTION SYSTEM DESIGN

The next step in the aerodynamic design study was the preliminary design of the swirl burners. The fan and ram burners in the STFRJ368 use the swirling flow combustion concept, which has been under investigation by P&WA for the past four years. Rig testing has demonstrated that swirling flow combustion provides stable, efficient burning in a much shorter length than conventional combustion systems. In addition, this type of combustion system provides a low lean blowout limit, and with proper fuel system zoning gives high combustion efficiency over a much wider range of fuel-air ratios than conventional systems.

The swirl burner uses the concept of centrifugal force generated by a rotating airflow to cause flame to propagate radially across the airstream at rates that may substantially exceed normal turbulent flamespeeds. The high rate of flame propagation is the result of the difference in the centrifugal forces acting on the dense unburned fuel-air mixture and the less-dense hot products of combustion.

The swirl combustion system designed for the STFRJ368 fan and ram burners consists of a swirl vane cascade, a set of spraybars and a pilot burner, as shown in figure 4. Both the fan burner and the ram burner employ this configuration. Each flow then exits to a common combustion duct just downstream of the fan and ram pilot burners. The aerothermodynamic design analysis performed for each burner included the definition of the swirl vane inlet Mach number, the determination of the required swirl angle, and the definition of the geometry of the swirl vanes, the pilot burner and the common combustion duct. In

addition, pressure losses were calculated for the swirl vane cascade, the mixing and expansion of the swirling flow downstream of the swirl vanes, and the loss due to heat addition in the combustion duct. The results of the analyses were expressed parametrically to allow trades between flowpath geometry and performance. This technique provides an integrated design that meets the required combustion efficiency at an allowable level of pressure loss, and maintains an acceptable engine envelope.
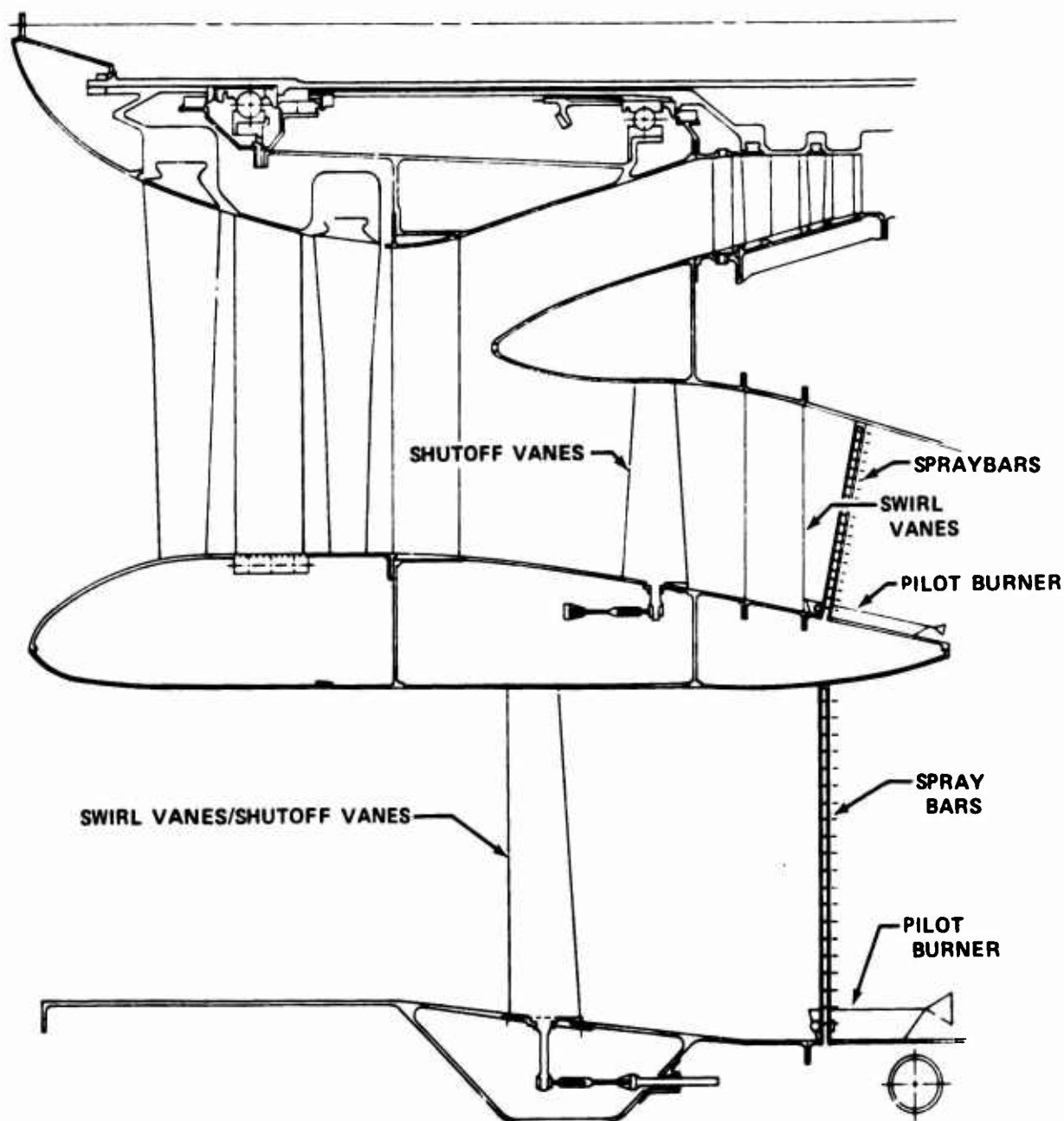

Figure 4. STFRJ368 Fan/Ram Duct   FD 73660

8

Figure 5 shows a parametric relationship between initial flamespreading angle and vane swirl angle as a function of combustion duct outer diameter. To meet reasonable engine envelope requirements, the duct outer diameter and length were established at 66.8 and 41.0 in., respectively. A maximum axial Mach number of 0.33 was established for the common combustion duct to provide acceptable fan/ram flow mixing characteristics during transition as well as acceptable hot gas pressure losses. This required a combustion duct area of 2800 sq in. which results in a combustion duct inner diameter of 30.3 in. To meet engine combustion efficiency requirements with this combustion duct geometry and a hot gas Mach number of 0.33 requires an initial flamespreading angle of 9 deg. From figure 5, an initial flamespreading angle of 9 deg and a combustion duct outer diameter of 66.8 in. (5.65 ft) requires a swirling flow angle of 49.5 deg for both the fan and ram combustors.
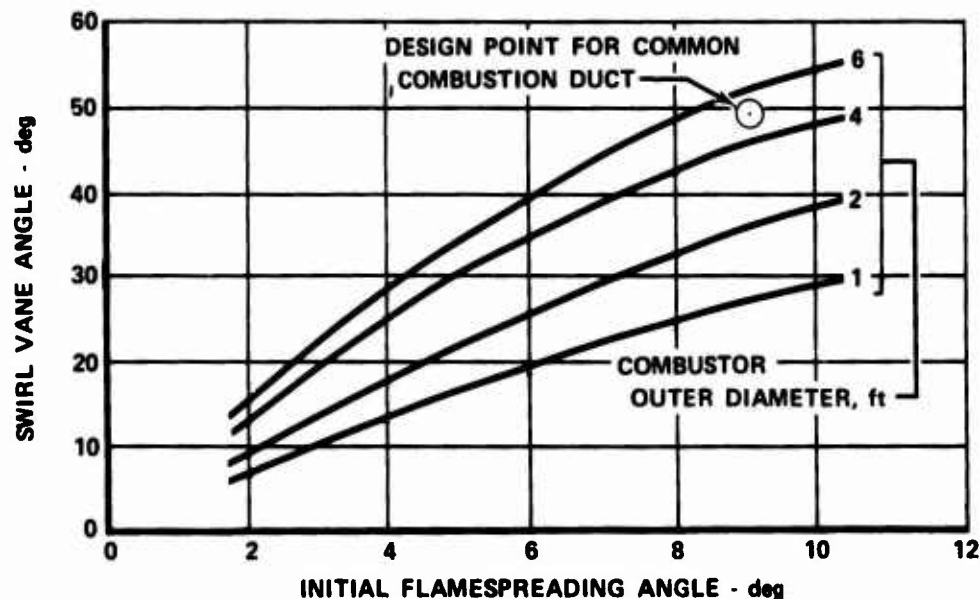

Figure 5. The Relationship Between Swirl Vane   FD 73661
Angle and Initial Flamespreading Angle
in Swirling Flow Combustion

Figure 6 shows the swirl vane geometry designed to provide 49.5 deg of swirl with a uniform pressure and mass flow distribution both radially and circumferentially. This design was generated using our turbine streamline design computer program, which has been used in the past to design swirl vane cascades for swirl burner rigs with excellent results. The swirl vane cascade design has 96 vanes with a constant vane section thickness of 0.050 in. in the fan duct, and 112 swirl vanes 0.125-in. thick in the ram duct, where the swirl vanes are also used as the shutoff vanes.

The pressure loss characteristics for the swirl cascades are shown in figure 7 as a function of cascade inlet Mach number. The fan cascade operates at a maximum inlet Mach number of 0.254 and the ram cascade operates at a maximum inlet Mach number of 0.220. Figure 8 shows the estimated total pressure loss associated with mixing and expansion of the swirling flow at the exit of the swirl cascade, for both fan and ram cascades, as a function of axial Mach number and swirl angle. This figure is applicable to both the fan and ram swirling flows.
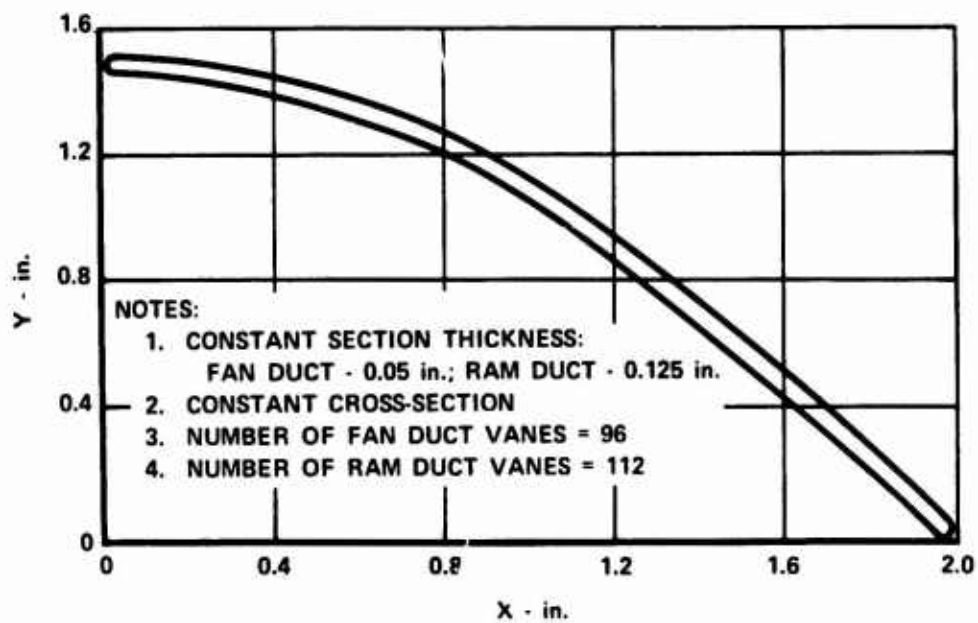
9

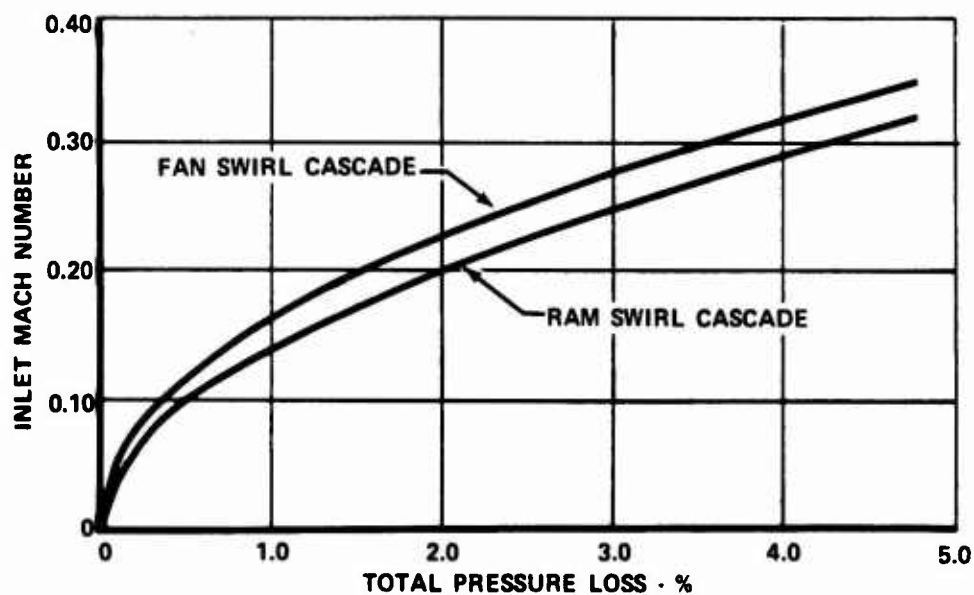Figure 6. STFRJ368 Swirl Vane Mean Section   FD 73662

Figure 7. STFRJ368 Fan and Ram Swirl Estimated   FD 73663
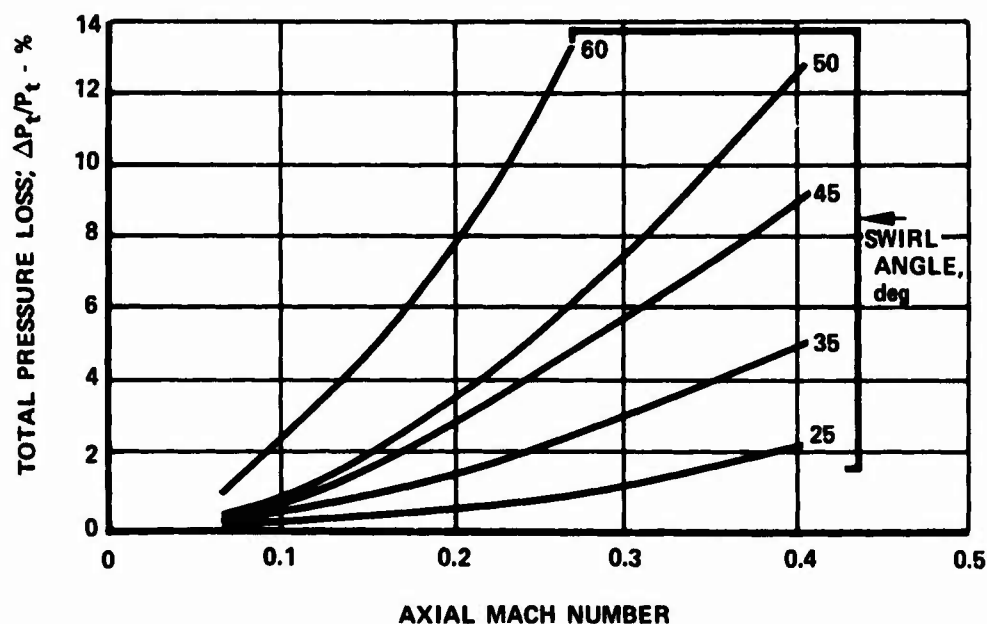Cascade Pressure Loss

10

Figure 8. STFRJ368 Swirling Flow Estimated   FD 73664
Total Pressure Loss

Table I summarizes the calculated total pressure losses for the fan and ram burners at various flight points. The pressure losses shown are the sum of the swirl cascade losses, the swirling flow mixing and expansion losses, and heat addition losses.

Table I. STFRJ368 Estimated Combustion System Pressure Loss

	Flight Point Alt, ft/Mach No.	Swirl Cascade Inlet Mach No.	Combustion System Pressure Loss $(\Delta P_t/P_t)$*
	80,000/4.5 (Cruise)	0.054	0.0076
	45,000/3.0 (Accel)	0.218	0.0980
Ramburner	37,000/2.5 (Accel)	0.220	0.1180
	75,000/3.0 (Maneuver)	0.218	0.0980
	61,500/4.5 (Max q at Max Mach)	0.112	0.0228
Fanburner	36,500/2.5 (Accel)	0.254	0.0808
	0/0 (SLTO)	0.222	0.0702

*Includes: Swirl cascade loss, swirling flow mixing and expansion losses, and heat addition loss.

11

In addition to swirl cascades, the fan and ram burners must each be provided with pilot burners. These burners are needed because the axial velocities exceed turbulent flamespeeds, and thus some form of pilot to ignite the incoming fuel-air mixture is needed, as in all burners. In conventional afterburners the recirculating hot gas behind the flameholders performs this function. In swirl burners a continuous pilot ring around the outer periphery of the burner generates a hot flame bubble, which is driven through the incoming fuel-air mixture by buoyancy, igniting the mixture as it passes through it. Each pilot burner in the STFRJ368 design occupies 10% of the burner duct areas; this allows up to approximately 7% of the duct flow to pass through each pilot when entrance losses and fuel nozzle blockage are considered. Rig testing of swirl burners has established that this is more than sufficient to provide the required flame piloting.

The preliminary design of the combustion systems did not require a detailed fuel system design analysis at this stage of the engine design. However, a preliminary analysis was done to provide assurance that the fuel system can be incorporated without penalty or compromise to the design. The preliminary analysis provided inlet manifold sizes, spraybar sizes, and number of spraybars and determined that these components were compatible with the aerodynamic design. The fan duct burner uses forty 0.30-in. diameter spraybars supplied by 1.3-in. diameter manifold whereas the ram duct uses sixty-four 0.30-in. diameter spraybars supplied from a 1.8-in. diameter manifold.

D.   FLOW FIELD DEFINITION

A streamline analysis of the fan duct flow field shown in figure 9 was made to ensure a stable, low-loss transition from the fan discharge plane to the fan duct burner. The study consisted of an analysis of the fan, fan duct, and high compressor inlet using our streamline analysis computer program. The blockage effects caused by the eight support struts were included in the analysis. A rotating fan blade immediately upstream of the strut-exit guide vane, and a rotating high compressor blade downstream of the strut trailing edge were modeled to include the effect of rotors on streamline definition. Fan discharge total pressure and total temperature profiles were estimated based on experimental data obtained from advanced fan rig tests at a comparable flowrate and fan pressure ratio. The flow was then turned 49.5 deg at the swirl vane trailing edge by the fan duct swirl vane cascade design as described in the previous section.

The results of the streamline analysis are presented in figures 10 and 11. Figure 10 shows the predicted fan discharge radial Mach number and total pressure profiles. The high pressure along the hub helps to minimize potential boundary layer separation tendencies and thus provide a more stable fan operation. Figure 11 illustrates the fan duct inner wall, outer wall, and mean velocity profiles, along with the average Mach number distribution down the length of the fan duct. The velocity characteristics show an acceleration of flow up to the minimum area plane (Station 4), then an overall deceleration through the 11.4 deg annular diffuser and the rear portion of the struts. The flow begins to reaccelerate through the swirl vanes (Stations 8 to 9) as a result of the change in flow direction and a 4.8% blockage. This swirl vector is maintained through the remainder of the fan duct. No separation problems are anticipated with this duct design.
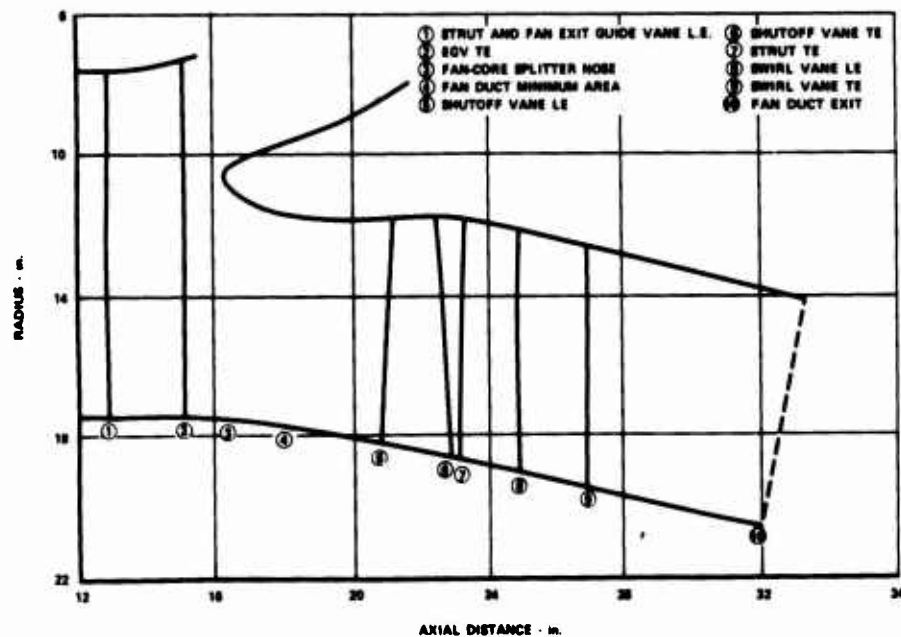
12

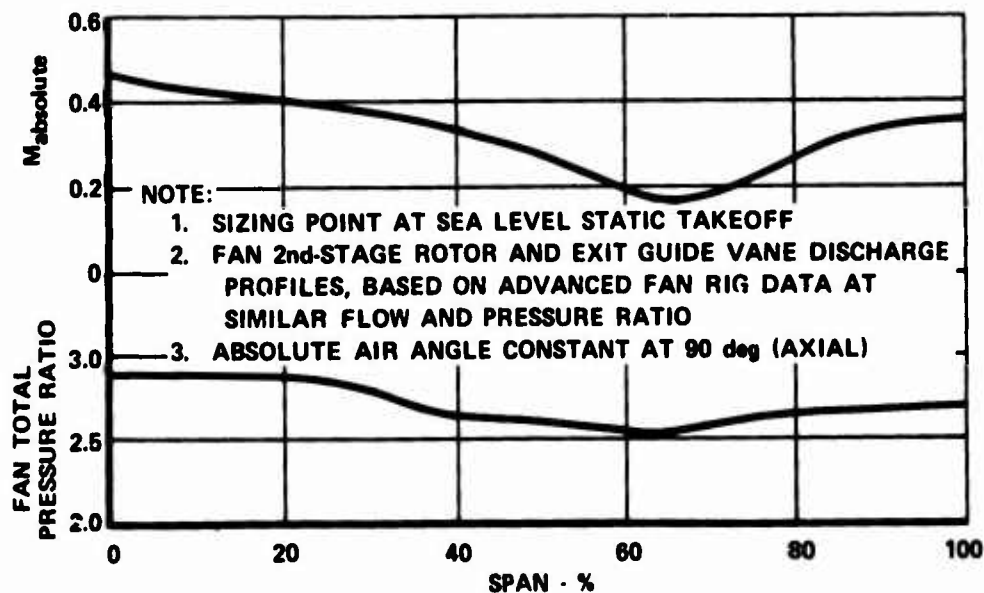Figure 9. STFRJ368 Fan Duct Flowpath   FD 73665

Figure 10. STFRJ368 Fan Discharge Radial Mach   FD 73666
            Number and Pressure Ratio Profiles
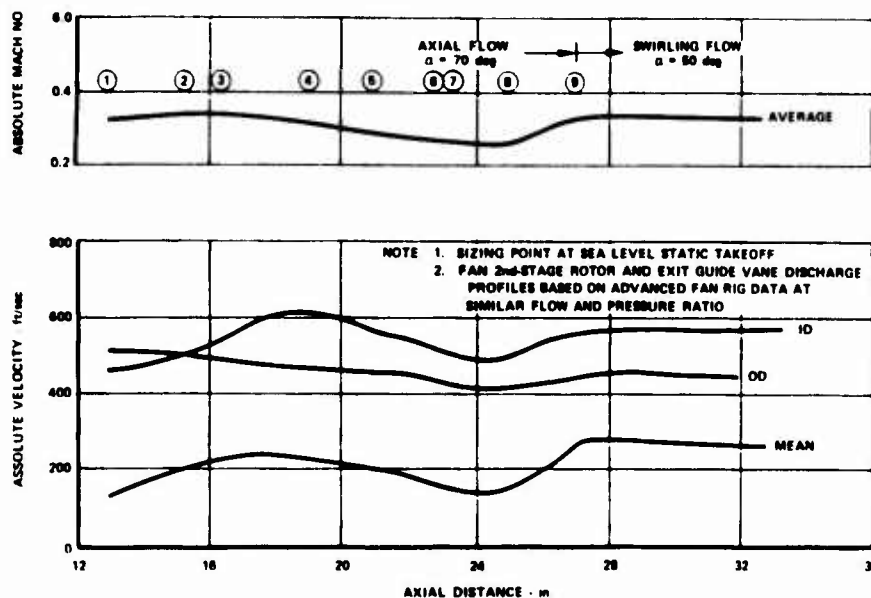
13

Figure 11. STFRJ368 Fan Duct Wall Velocity and   FD 73667
          Average Mach Number Profiles

E. PRESSURE LOSSES

Pressure losses in the fan/ram duct are cau   d by skin friction, the sup-
port struts, diffusion, and the shutoff vanes. Pressure loss coefficients were
estimated for each of these loss mechanisms and are presented in table II.
Table III presents the overall combustion system and aerodynamic pressure
losses obtained by adding the combustion system losses from table I to the
aerodynamic losses calculated at each flight condition. Duct Mach numbers
were calculated at locations upstream of the shutoff vanes in both fan and ram
ducts. In general, the maximum pressure losses occur near the 37,000/2.5 point
and are nearly the same magnitude (10-12%) for both fan and ram operation.

The support strut pressure loss characteristics in both the fan and ram
ducts were calculated using our cascade loss computer program. The basis of
this program is a correlation of experimental test data from cascades of various
gap-chord ratios, thickness-to-chord ratios, inlet and exit metal angles, airfoil
series number and the inlet Mach number and air angle. The fan side strut,
a symmetrical, noncambered 400 series airfoil with a 0.929 gap-chord ratio and
a 12% thickness-to-chord ratio, has a pressure loss coefficient ($\Delta P/q$) of 0.0152
for inlet air angles between 77 and 103 deg. Beyond these two angles, loss in-
creases rapidly because of severe flow separation on the airfoil surface. Since
the strut leading edge and fan exit guide vane leading edge are located in the same
plane, the fan second rotor will have to be designed so that the rotor discharge
absolute air angle stays within the 77 to 103 deg range. This design requirement
will ensure a low-loss strut and consequently, high component efficiency.

The ram side support struts are identical to the fan side except for a higher
gap-chord of 2.06, (because of the increased radius) and a flat, nonswirling,
axial air angle profile at its leading edge. The pressure loss coefficient ($\Delta P/q$)
is constant at 0.007 for air angles between 89 and 101 deg.

14

Table II. Estimated Pressure Loss Coefficients

Component	Pressure Loss Coefficient, $\Delta P/q$
Fan Duct Struts	0.015
Ram Duct Struts	0.007
Fan Duct Diffuser	0.021
Ram Duct Diffuser	0.024
Fan Duct Skin Friction	0.006
Ram Duct Skin Friction	0.010
Fan Duct Swirl Vanes	0.60
Ram Duct Swirl Vanes	0.720

Table III. STFRJ368 Aerodynamic and Overall Pressure Losses

	Flight Point Alt, ft/Mach No.	Duct Mach No.	Aerodynamic Pressure Loss $(\Delta P_t/P_t)$*	Overall Pressure Loss $(\Delta P_t/P_t)$**
Ram Duct & Burner	80,000/4.5 (Cruise)	0.058	0.0001	0.0077
	45,000/3.0 (Accel)	0.220	0.0016	0.0996
	37,000/2.5 (Accel)	0.221	0.0016	0.1196
	75,000/3.0 (Maneuver)	0.219	0.0016	0.0996
	61,500/4.5 (Max q at Max Mach)	0.118	0.0005	0.0233
Fan Duct & Burner	36,500/2.5 (Accel)	0.299	0.0225	0.1033
	0/0 (SLTO)	0.271	0.0222	0.0924

*Includes: Strut Loss, Skin Friction Loss, and Annular Diffuser Loss in Both Ram and Fan Ducts; Shutoff Vane Loss in Fan Duct Only

**Includes: Aerodynamic Loss Plus Combustion System Loss Shown in table I.

The duct pressure loss resulting from skin friction was calculated using standard formula for compressible flow in pipes. In both the ram and fan ducts, the friction coefficient was estimated to be on the order of 0.008 for the

low roughness of rolled sheet metal. The fan duct pressure loss coefficient, defined from the minimum area plane to the swirl vane leading edge, was 0.006, and the ram duct pressure loss coefficient, defined from the fan-ram splitter to the strut trailing edge was 0.010.

The diffuser pressure loss was estimated from NACA experimental data: the fan side annular diffuser with an area ratio of 1.147 and a total equivalent conical angle of 11.4 deg results in a loss coefficient of 0.021. The ram side diffuser with an area ratio of 1.169 and a total equivalent conical angle of 8.1 deg results in $\Delta P/q = 0.024$.

The fan duct shutoff vane pressure loss characteristics are presented in figure 12 as a function of flow parameter. These characteristics were estimated based on orifice pressure loss data. In the open position ($A_2/A_1 = 0.9$) the vanes operate at a flow parameter of 0.25 with a corresponding pressure loss of 2%. As the vanes begin to close down, the value of the throat flow parameter begins to increase because of the reduction in flow area. At some point the vanes will have closed down so that they no longer act as airfoils but more like a series of nozzles and diffusers, with still a relatively low loss level. Further turndown causes the vanes to act as orifices with an increase in loss. Eventually the vanes will have closed sufficiently that the flow readily passes through the ram duct resulting in a reduction in the vane flow parameter and a decrease in loss. The actual definition of loss as the vane closes is a function of the turbofan engine shutoff scheme, the ram duct flow conditions, and the fan duct shutoff vane area transition schedule. This loss will be calculated during dynamic simulation of the engine system.

The results of the aerodynamic design study were incorporated into a preliminary design layout with details of the fan/ram duct flowpath, shutoff doors, support struts, swirl vanes, and swirl burners. This layout provides an update of the STFRJ368 engine with fan/ram duct components sized correctly for the selected design conditions.
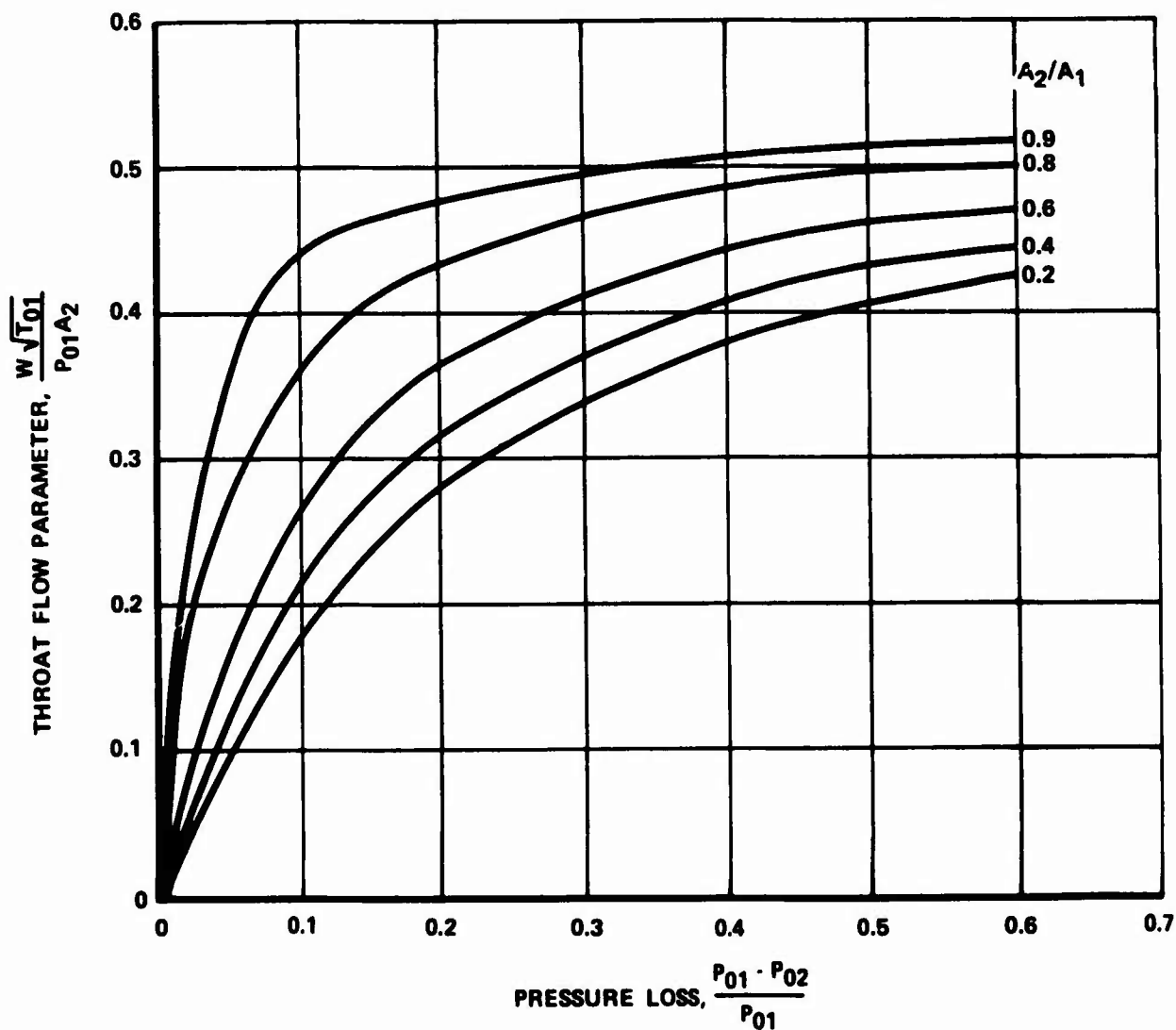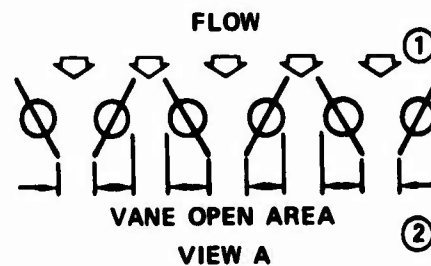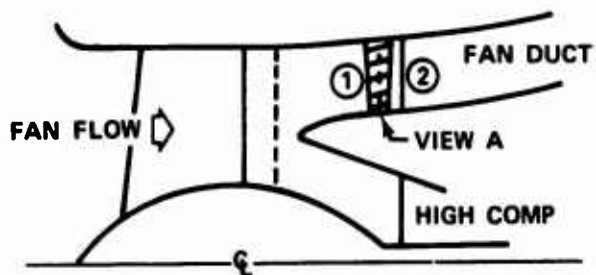
Figure 12.   Estimated STFRJ368 Fan Duct Shutoff   FD 73668
             Vane Pressure Loss in the Partially
             Closed Position

SECTION IV

TEST RIG DESIGN

A.   GENERAL

Design of the fan/ram duct test rig was initiated by scaling the STFRJ368 engine fan/ram duct design to fit the fixed dimensions of an existing small-scale fan model, shown in figure 13, which will be used to simulate the fan. A scale factor of 0.1167 was obtained by ratioing the fan tip diameter of the fan model to the fan tip diameter of the STFRJ368; hence, the scale of the test rig will be between 1/8 and 1/9 that of the full-scale engine.

The next step in the design was to study different methods of reducing the influence of the large fan model support strut on the swirling flow in the fan and ram ducts. Preliminary proposal sketches of the test rig showed this large strut extending all the way across both the fan and ram ducts. However, when the full-scale fan/ram duct design was scaled to model size, it was found that the swirl vanes in both ducts were located near the leading edge of the large strut. This single large strut would therefore have produced substantial blockage of the swirling flow in both the fan and ram ducts. The solution to this problem, as shown by the test rig sketch in figure 14 was to supply bearing lubrication oil and turbine drive gas (nitrogen) to the fan model through small, individual tubes. The portion of the large strut that remains in the fan duct is an integral part of the fan model and cannot be removed. By using the small individual tubes, however, the amount of blockage in the ram duct can be significantly reduced from that of a solid strut. Nevertheless, wakes of the supply tubes will still occur; instrumentation located downstream of the supply tubes was therefore, positioned to avoid the wakes.

To reduce the number of rig disassemblies during testing, it was desirable that the fan duct shutoff vanes be controlled from outside the rig. To accomplish this outside control, the fan vanes were relocated to the same axial station as the ram vanes and the same number of vanes are used in both fan and ram ducts, as shown in figure 14. In so doing, the fan vane control shafts can be located inside the ram vanes so that no additional blockage is added to the ram duct. To position the fan and ram duct vanes at the same axial location, the length of the fan duct was increased somewhat. However, since the test rig has a smaller number of vanes than the full-scale design, the relative chord length of the vanes must be greater; therefore, the increased fan duct length will accommodate the longer vanes.

To reduce the number of moving parts, fixed ram duct vanes were used rather than adjustable vanes. The decision to use fixed ram duct vanes was based on the transition studies that indicated that only two vane positions, open and closed, are needed, that is, the ram flow will not be throttled. The vanes will be fixed in the open position while the closed position will be simulated by a blocker plate installed in the ram duct as indicated in figure 14. Another simplification is the use of individual control quadrants rather than a synchronization ring to position the fan duct shutoff doors. This provides two benefits: reduction of complexity and hence fabrication cost, and the capability of producing clockwise swirl, counterclockwise swirl, and blockage-without-swirl with the same shutoff doors, as shown in figure 15. Tests with swirl in both directions are planned in order to evaluate the mixing and dump losses with the fan duct flow both co-rotating and counter-rotating with the ram duct flow. The fixed fan duct swirl vanes will be removed when the fan shutoff doors are used to generate swirl.

18
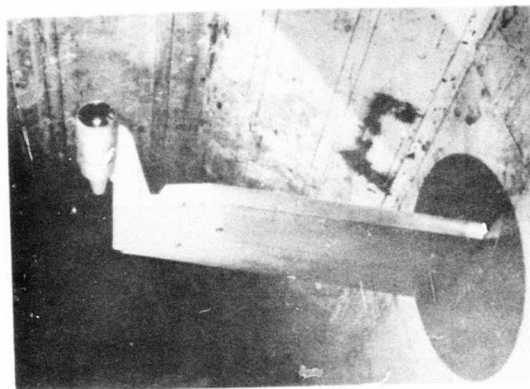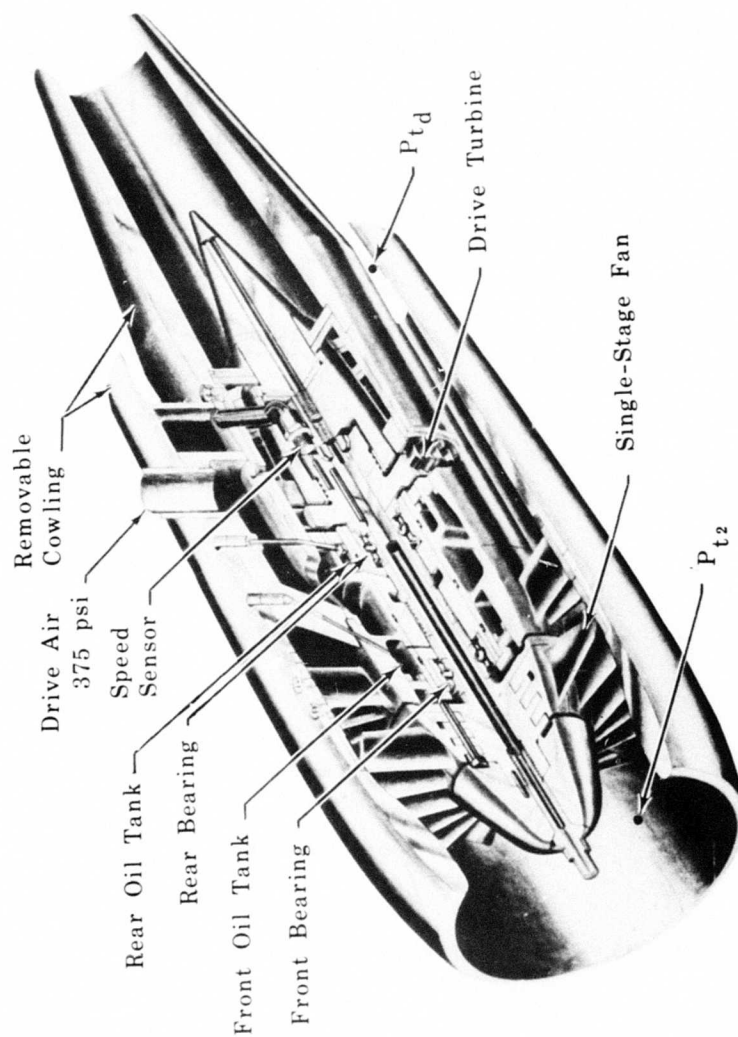
ISOLATED TEST SYSTEM

FD 23716

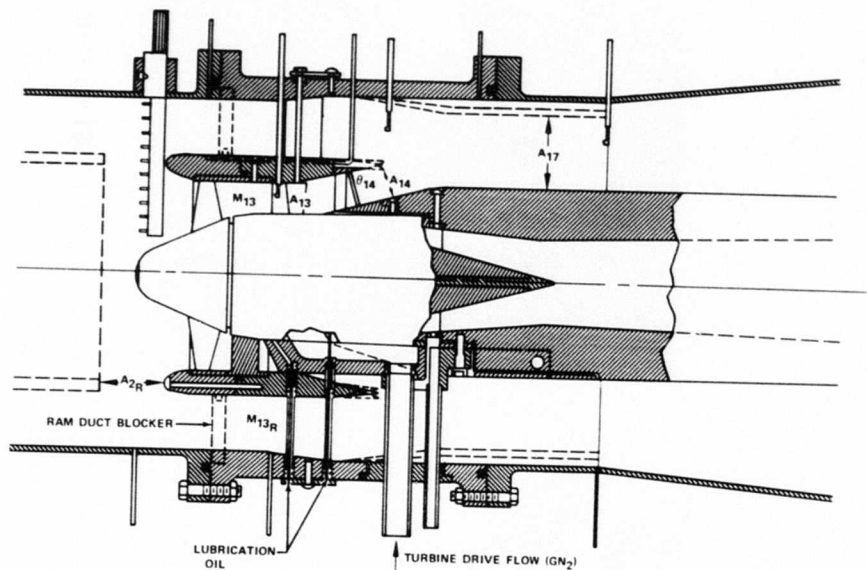Figure 13. Air—Powered Engine Model

19

Figure 14. Fan/Ram Duct Test Rig
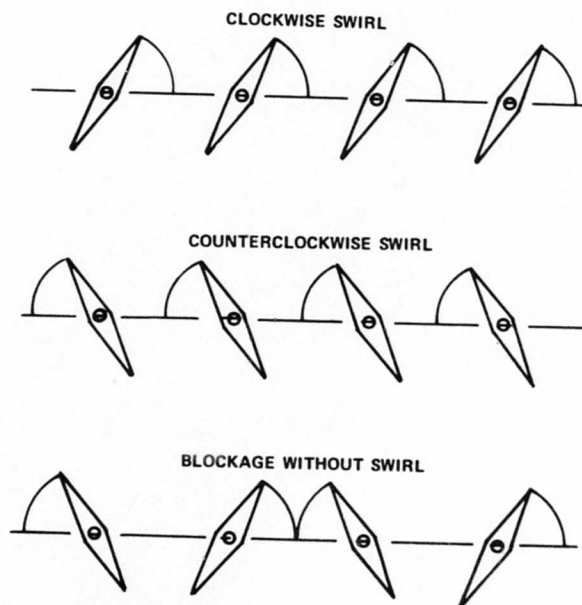
FD 73742

Figure 15. Fan Shutoff Door Positions

FD 73743

To properly simulate the flow spreading and mixing characteristics of the full-scale engine in the small-scale model, the centrifugal force field in the model must be similar to that of the full-scale engine. Hence, the swirl angle was reduced from 49.5 deg in the full-scale engine to 26.5 deg in both the fan and ram ducts of the model to keep the centrifugal force field the same. Cross sections of the fan and ram duct fixed swirl vanes are shown in figure 16 and the location of these and other rig parts are called out on the assembly drawing, figure 17.

The strut and vane blockage of the test rig is compared with that of the full scale engine design in table IV, wherein it can be seen that the rig has slightly more blockage than the engine. Blockage is calculated as the reduction in annulus cross-sectional area because of the swirl vanes, shutoff doors and struts, and was calculated at the midchord position. In the calculations for the engine, the blockage of the eight core-engine support struts is included in the shutoff door blockage. The test rig lubrication oil and GN_2 supply lines are not included in the blockage calculations because they are local blockages and will not influence the measurements.
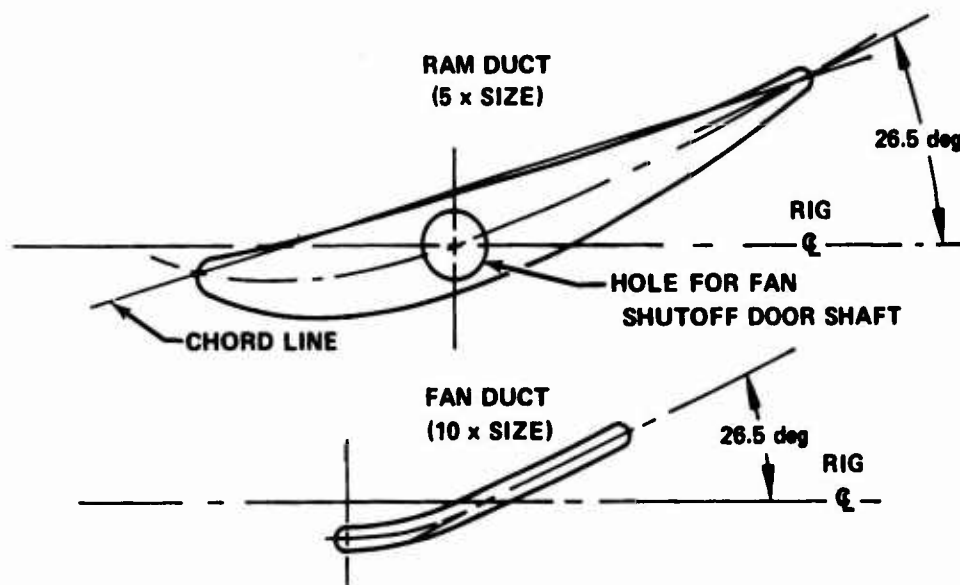

Figure 16. Swirl Vanes   FD 73744

Figure 17. Fan/Ram Duct Rig Assembly

GKJ 2017

22

Table IV. Comparison of Model and Engine Blockages

| Location | Blockage - % | |
	Test Rig	STFRJ368 Engine Design
Fan Duct Shutoff Doors	16.8	13.6
Fan Duct Swirl Vanes	7.5	7.3
Ram Duct Shutoff Doors	17.7	15.0

B.   TEST SETUP

The test facility setup, shown in figure 18, was designed to measure and control the airflow through the fan/ram duct rig with a minimum reduction in total pressure from friction and dump losses. Total flowrate will be measured by the low-loss, long-radius ASME bellmouth, and a conical diffuser is used to recover most of the dynamic pressure, or "q", that would be lost if the bellmouth flow were dumped into the inlet duct. An inlet screen is also fitted to prevent ingestion of foreign objects. Downstream of the rig, diffusers are provided to improve the pressure recovery for both rig flow and fan drive turbine discharge flow. This diffuser-within-a-diffuser was necessary to reduce the turbine backpressure to less than 10 psig in order to obtain the desired speed within the maximum allowable turbine supply pressure of 700 psig. The plenum, which includes the outer wall of the annular diffuser, connects the rig to the fans and houses the turbine exhaust elbow and discharge lines. During fan duct operation without ram flow, flow through the axivane fans will be blocked to control fan pressure ratio. During fan/ram and ram operation, the axivane fans will be in operation and will be throttled at the discharge end to control airflow through the rig.

Pressure, temperature, and air angle instrumentation is provided in the rig, as shown in figure 17. Total pressures and total temperatures will be measured at four axial stations: (1) at the inlet to the rig, (2) behind the fan exit guide vanes, (3) at the flow splitter exit, and (4) at the end of the simulated combustion chamber. A fixed rake will be used at the first station whereas cobra probes, which also measure air angle, will be used at the other three stations. Static pressure taps will be installed at each axial station and at several intermediate stations to indicate changes in wall pressures and centrifugal force field.

During detailed design of the rig parts, simple construction techniques and loose tolerances were used where possible to minimize fabrication costs. The inlet P_t/T_t rake will be fabricated, but all other instrumentation will be purchased off-the-shelf. Materials specified were fiberglass for the inlet bellmouth and conical diffuser and AISI 347 stainless steel for all other parts. Detailed manufacturing drawings of all the parts were prepared and checked - all parts are now ready for procurement. No problems were encountered in designing the rig around the existing fan model.
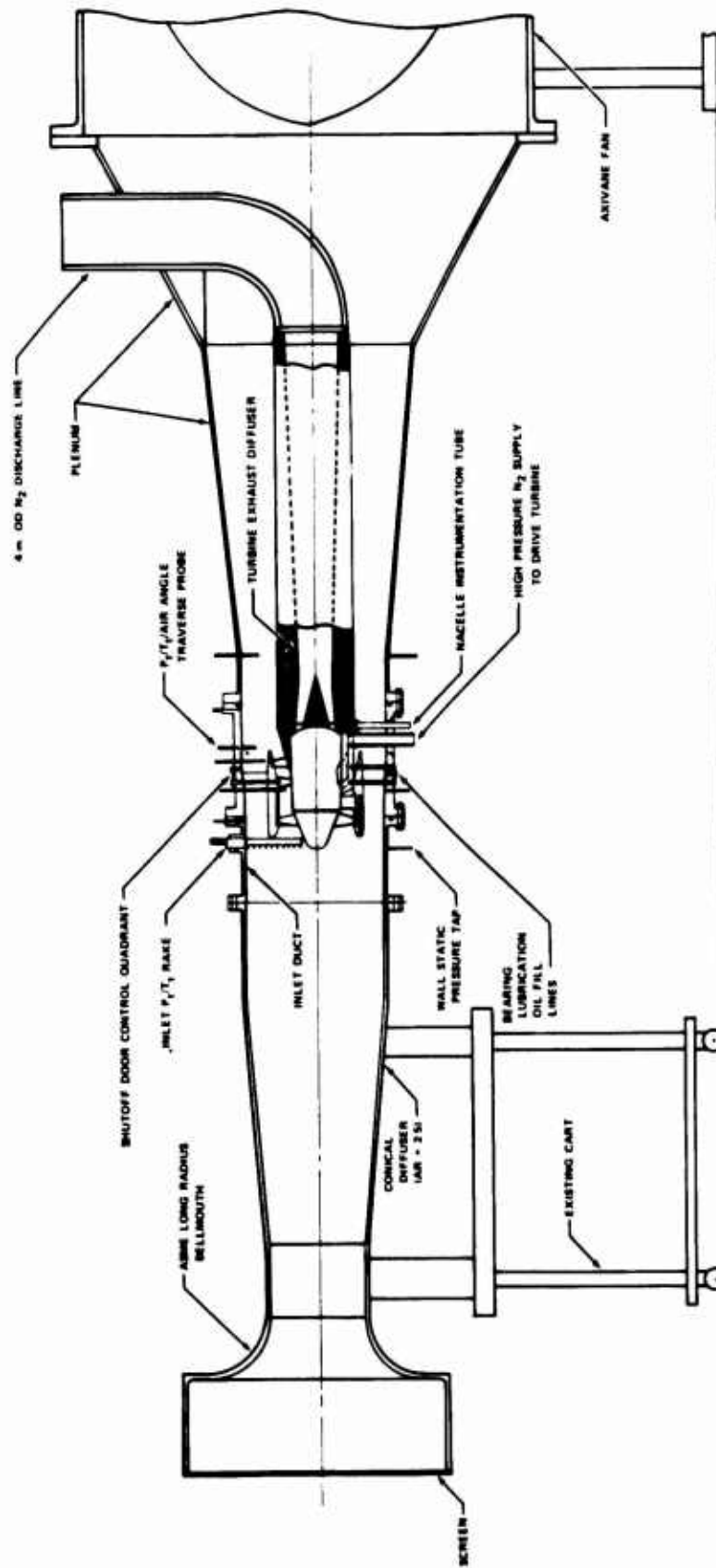
Figure 18. Fan/Ram Duct Model Test Facility

FD 73746

24

The final design configuration pro des for varying the following aero-dynamic and geometric parameters (also illustrated in figure 14):

Fan and ram duct Mach numbers, M_{13} and M_{13R}

Fan speed, N_1

Fan pressure ratio, PR_f

Fan duct exit area, A_{14}

Fan duct shutoff door area, A_{13}

Fan duct swirl angle, θ_{14}

Combustion chamber area, A_{17}

A sufficient number of parts were designed to permit testing each variable at three or more levels. Procurement of the rig parts, testing of the above variables, and analysis of results are planned to be accomplished under Phase II of this program.

SECTION V

ENGINE DYNAMIC SIMULATION

A. GENERAL

A dynamic simulation of an engine is the primary tool used in analyzing engine operational characteristics and controls. These characteristics are especially important in a combination-cycle engine because a combination-cycle engine has a large number of control variables that must be programed and scheduled correctly to achieve smooth, stable transitions from turbofan to ramjet, and vice-versa. A dynamic simulation of an engine includes mathematical models of all engine components, plus the dynamic relationships needed to describe the transient behavior of the engine. In this manner, the dynamic response of an engine to various control inputs is accurately described. Hence, with the simulation as a tool, the control system and logic necessary to achieve the desired propulsion system response, e.g., a smooth transition, is easily developed. Under the Phase I effort described herein, such a dynamic engine simulation was formulated and checked out so that it would be ready for the transition control studies planned for Phase II of this program. No control studies were conducted during Phase I; the transient transition test cases presented in this report only demonstrate that the computer program is operational. They do not represent optimized transitions.

B. SIMULATION DESCRIPTION

The STFRJ368 engine simulation is made up from separate component simulation modules. Each engine component module contains the aerothermodynamic equations that characterize the corresponding engine component.

Transient modules contain the logic to calculate engine dynamics and to control the program's input and output during transients. The input-output modules contain the logic to read program inputs and print output parameters. Output parameters can also be stored for later processing, such as display on graphics equipment or plotting. A main program ties together the engine components, transient, and input-output modules.

The specific arrangement of the simulation components, presented in figure 19, shows how the calculation flowpath of the simulation is similar to the actual particle flowpath in the engine. Each component accepts the required inputs from upstream components and supplies necessary output to the down-stream component. This one-to-one aerodynamic and thermodynamic similarity provides a better understanding of actual engine operation.

The simulation performs calculations concurrently, even though the equations are solved in the order in which they are arranged in the program. The program stops time, performs all calculations in the steady-state mode, then advances time by a given increment and repeats the same steps. The dynamic path is de-scribed through a large number of such calculations, and is piece-wise continuous.
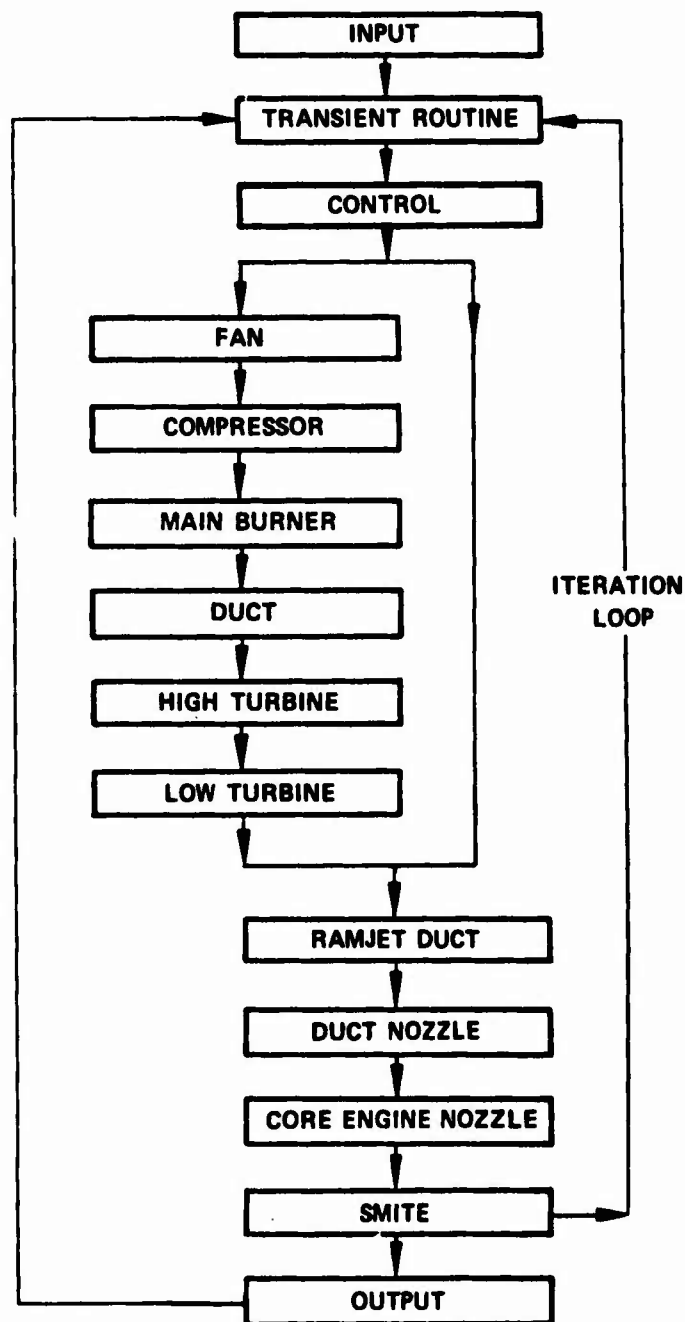
Figure 19. STFRJ368 Simulation Flowchart   FD 73748

C. ENGINE COMPONENT DESCRIPTION

The simulation treats each component as a separate entity described by gas dynamic relationships that relate inlet and exit pressures, temperatures, and gas flows, as illustrated by figure 20.

Engine component characteristics are derived from analytical and empirical techniques. As component test data become available, these performance characteristics will be revised to improve the engine dynamic representation. The following is a brief description of the main engine simulation components.

FAN

$$\frac{PR\text{-}1}{PR_d\text{-}1}$$

$N_1/\sqrt{2}$

θ_2

COMPRESSOR

$$\frac{PR\text{-}1}{PR_d\text{-}1}$$

$N_2/\sqrt{\theta 2.4}$

$$W_a\sqrt{\frac{\theta 2.4}{\theta 2.4}}$$

COMBUSTOR

T

ΔT

W_f/W_a

HIGH-PRESSURE TURBINE

$$\frac{(W\sqrt{T/P})}{(W\sqrt{T/P})_d}$$

$$\frac{(W\sqrt{T/P})}{(W\sqrt{T/P})_d}$$

$P_t4.4/P_t4$

HIGH-PRESSURE TURBINE

$$\frac{\eta}{\eta_d}$$

$$\frac{(\Delta H/T)}{(\Delta H/T)_d}$$

N_2/N_d

FAN TURBINE

$$\frac{(W\sqrt{T/P})}{(W\sqrt{T/P})_d}$$

$$\frac{(N/\sqrt{T})}{(N/\sqrt{T})_d}$$

$$\frac{(P/P\text{-}1)}{(P/P\text{-}1)_d}$$

FAN TURBINE

$$\frac{\eta}{\eta_d}$$

$$\frac{(\Delta H/T)}{(\Delta H/T)_d}$$

$$\frac{N_1}{N_{1d}}\sqrt{\frac{\Delta H_d}{\Delta H}}$$

DUCT DOOR

A_1/A_2

$$\frac{W\sqrt{T}}{PA}$$

$$\frac{P_1 - P_2}{P_1}$$

DUCT PRESSURE LOSS

$$\frac{\Delta p}{P}$$

MACH NO.
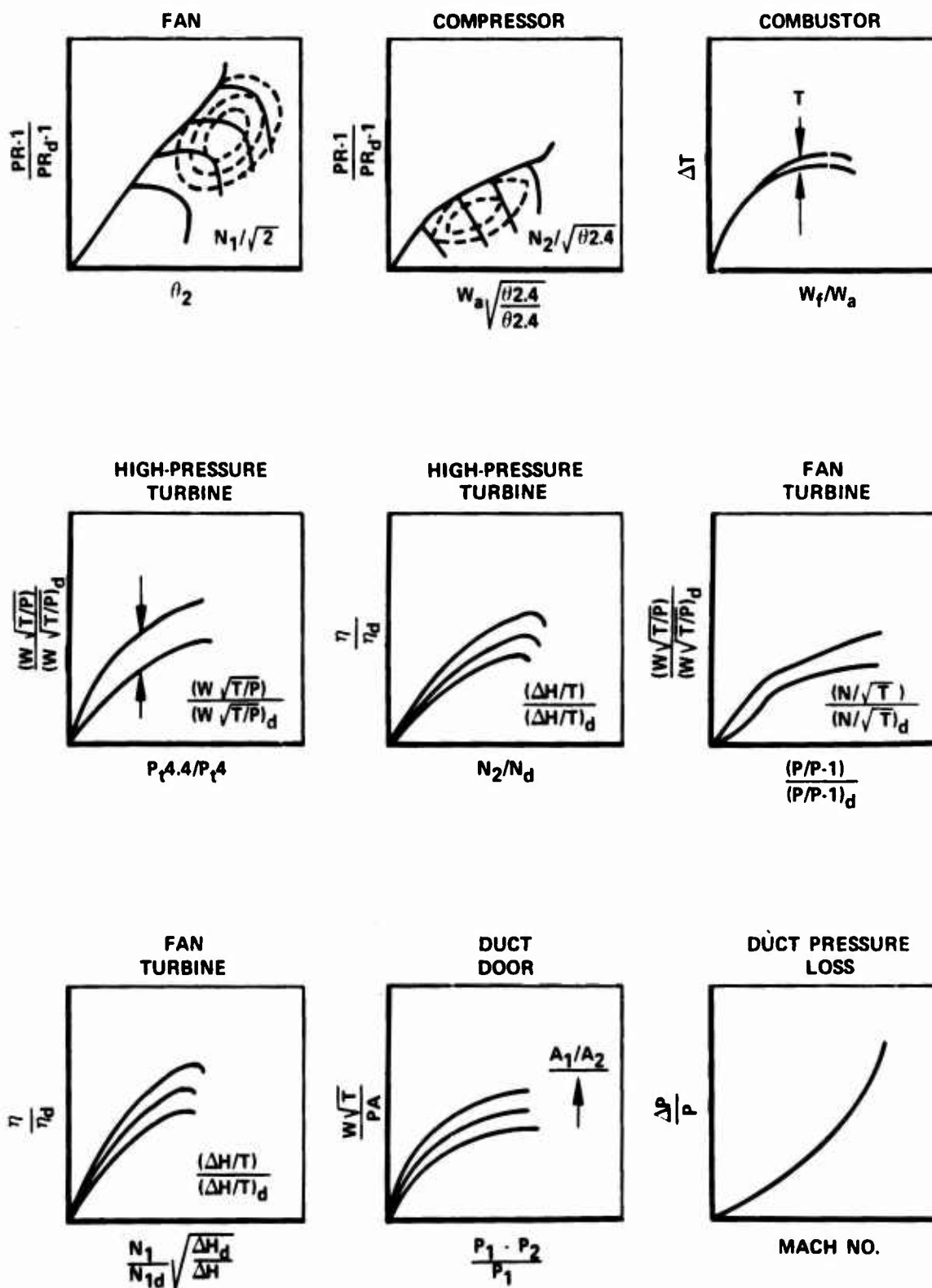
Figure 20. STFRJ368 Major Engine Components   FD 73749

28

1. Fan

Fan operation is described by a map that relates corrected airflow, efficiency pressure rise and corrected speed, (see figures 21a and 21b). The map variables are nondimensional to allow scaling. The fan is evaluated with fan M-line and rotor speed. (An M-line is the locus of points of a constant value of pressure rise divided by corrected airflow on a fan or compressor map. An operating point is thus uniquely defined by the intersection of an M-line and a rotor speed line.) These two parameters determine fan efficiency and hence the fan operating point. Inputs to the fan subroutine then are fan inlet total pressure and temperature, rotor speed and M-line. Outputs are gas flow, exit total pressure and temperature, efficiency, and required power.

The degree of fan stability is expressed by the fan surge margin calculated by the following equation:

$$\frac{\left(\dfrac{\text{Pressure Rise}}{\text{Corrected Airflow}}\right)_{\text{surge}} - \left(\dfrac{\text{Pressure Rise}}{\text{Corrected Airflow}}\right)_{\text{operating}}}{\left(\dfrac{\text{Pressure Rise}}{\text{Corrected Airflow}}\right)_{\text{operating}}}$$

The surge line is shown on the fan map in figure 21a whereas the operating point is calculated by the dynamic simulation.

2. Compressor

The compressor operation is identical to that of the fan. The compressor map is shown in figures 22a and 22b.

3. Combustor

The combustion process is described by bivariate functions that determine burner temperature rise from inlet temperature and fuel air ratio. Efficiency is calculated as a function of fuel-air ratio. The same subroutine is used for the main engine, fan duct, and ram duct burners. For given burner inlet conditions the subroutine has three modes of operation. Combustion can be simulated by specifying fuel-air ratio, fuel flow, or burner temperature. The other two parameters are then calculated. Total pressure losses because of heat input are calculated from Rayleigh line and friction loss relationships. A typical temperature rise curve is shown in figure 23.

4. Fan Duct

Duct pressure loss is calculated from compressible flow relationships using empirical friction coefficients. Door pressure loss is described by a bivariate function that relates pressure drop to door area and flow parameter, as shown in figure 24. (This is the same function previously shown in figure 12.) Inputs are duct inlet total temperature, pressure, and gas flow. Outputs are total temperature, pressure, and gas flow.
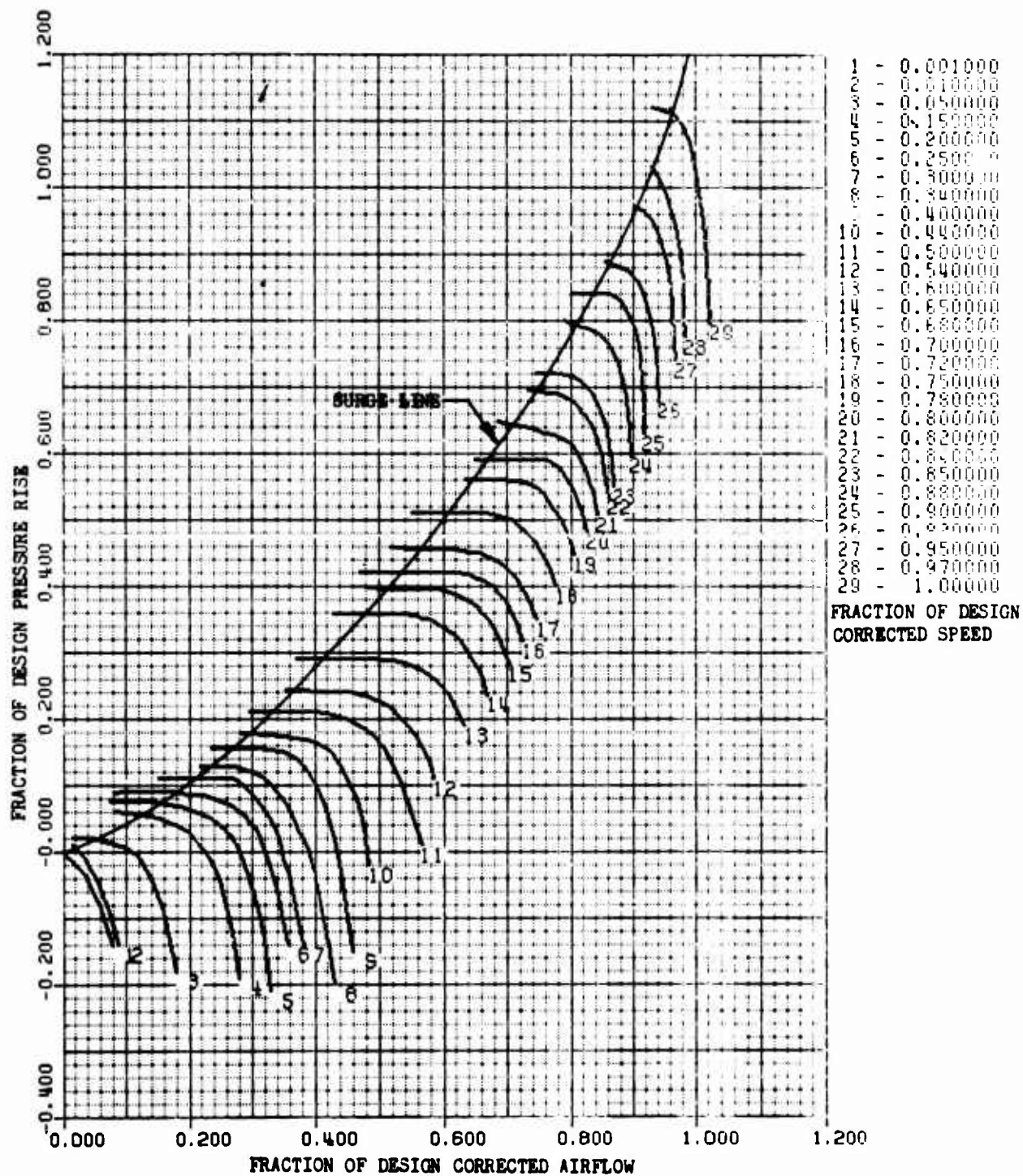
Figure 21a. STFRJ368 Turbofan Ramjet Fan Map
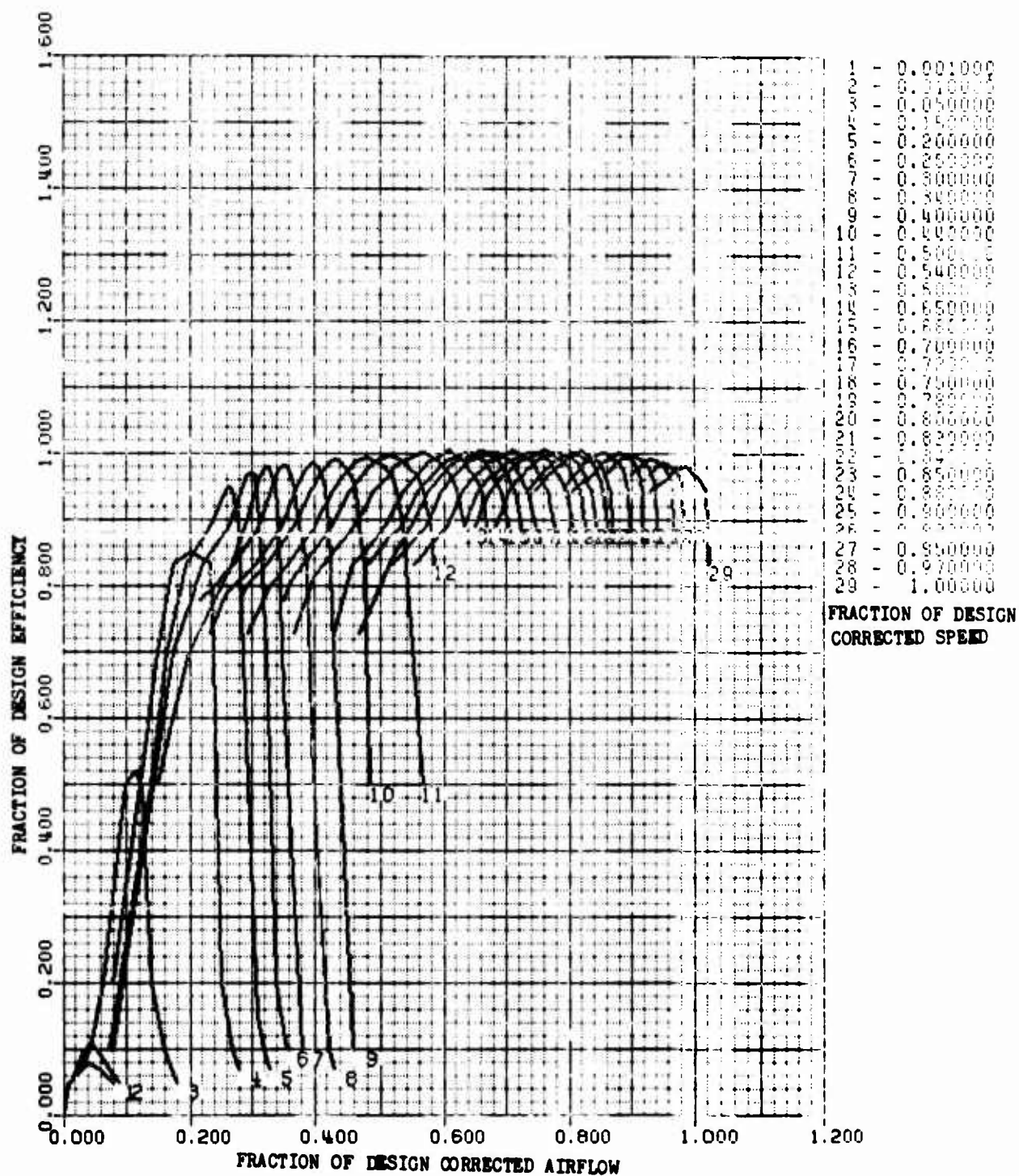
Figure 21b. STFRJ368 Turbofan Ramjet Fan Map (Continued)
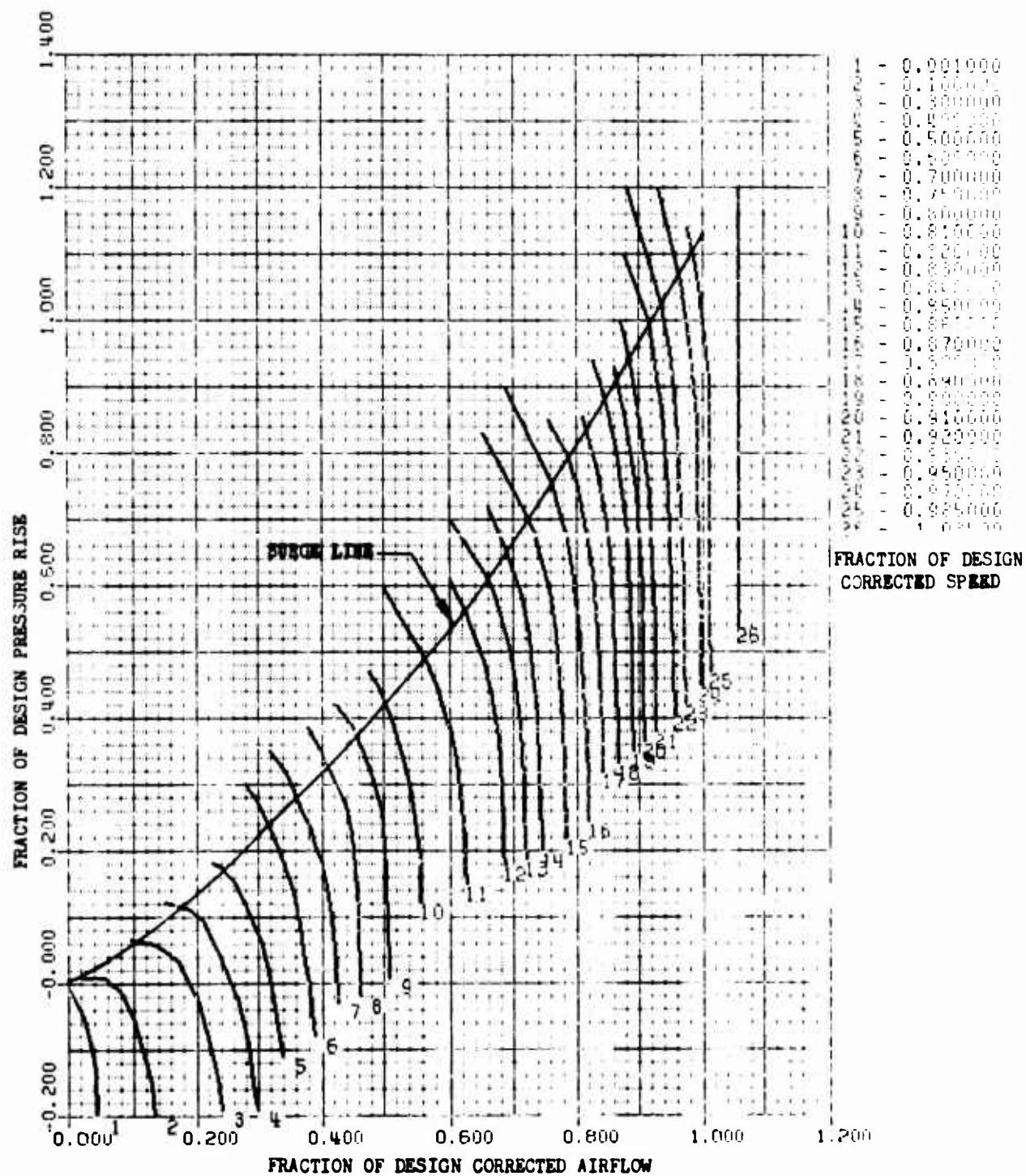
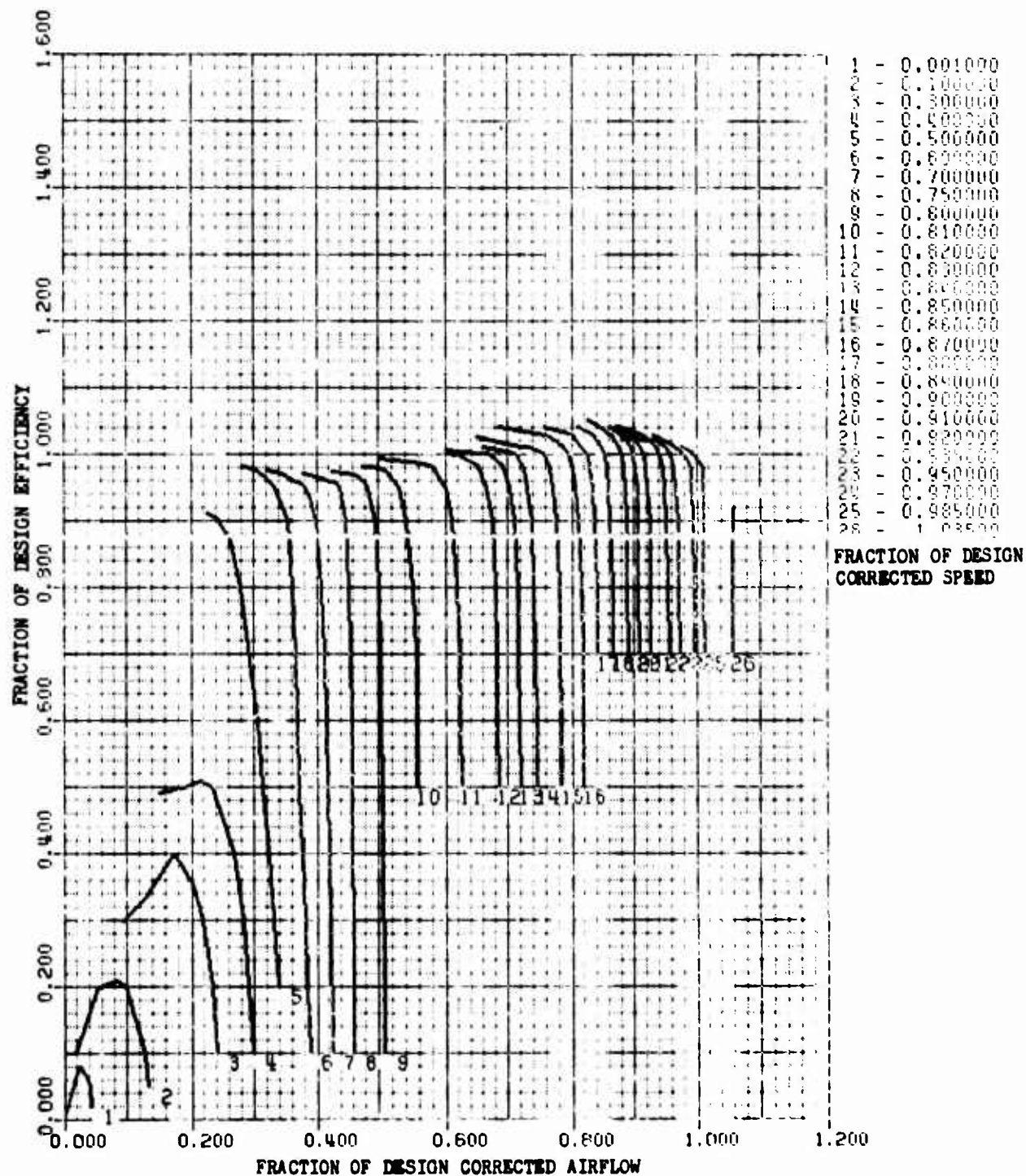Figure 22a. STFRJ368 Turbofan Ramjet High
Pressure Compressor Map

Figure 22b. STFRJ368 Turbofan Ramjet High
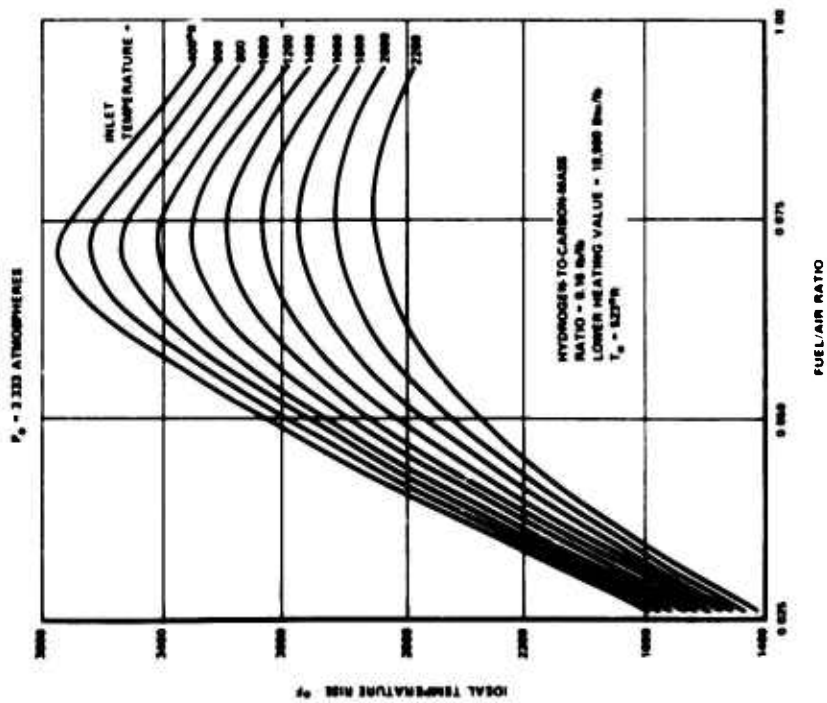Pressure Compressor Map (Continued)

Figure 23. Ideal Temperature Rise for   FD 73750
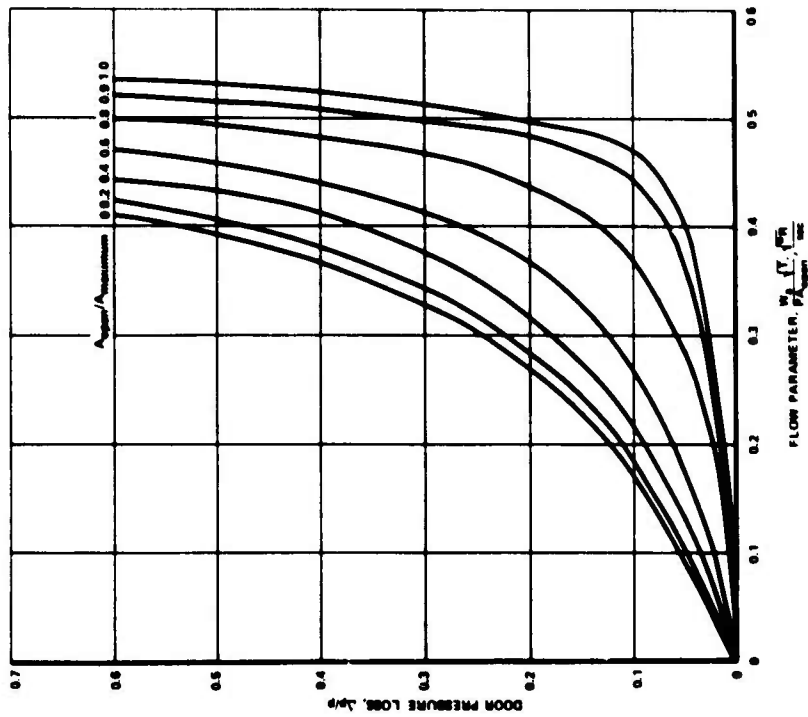Constant Pressure Combustion
of Hydrocarbon Fuels

Figure 24. STFRJ368 Estimated Shutoff   FD 73741
Door Pressure Loss

5. High Turbine

High turbine characteristics are represented by two bivariate functions
(see figures 25 and 26). The first relates inlet flow parameter to total pressure
drop and corrected rotor speed. The second describes the relationship between
efficiency, ideal work and rim velocity ratio (a function of rotor speed and turbine
enthalpy drop). Turbine efficiency is also corrected for Reynolds number effects.
Inputs to the subroutine are inlet total pressure and temperature, rotor speed,
gas flow, and required compressor work. Outputs include exit total temperature
and pressure ratio.

6. Low Turbine

Low turbine characteristics, identical in form to those of the high turbine,
are shown in figures 27 and 28.

7. Ram Duct

Duct pressure losses are calculated from compressible flow relationships
using empirical friction coefficients. Door pressure loss is described by a
bivariate function which relates pressure drop to door area and flow parameter,
figure 24. Inputs are ramjet inlet total pressure and temperature and corrected
flow. Outputs include total temperature and pressure and gas flow.
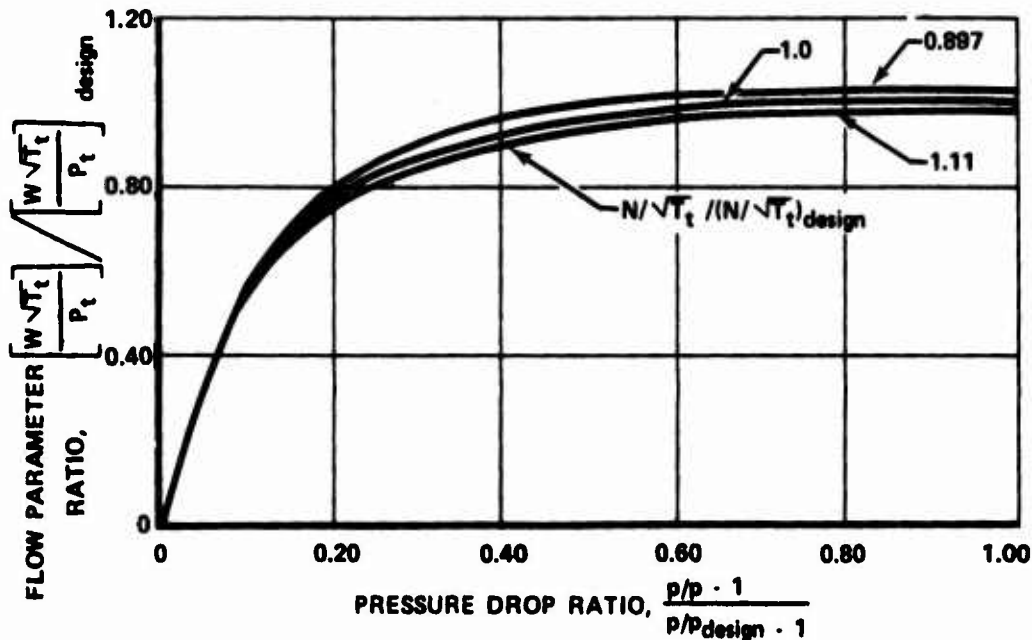
Figure 25. STFRJ368 High Pressure Turbine   FD 73745
Flow Parameter vs Pressure Ratio
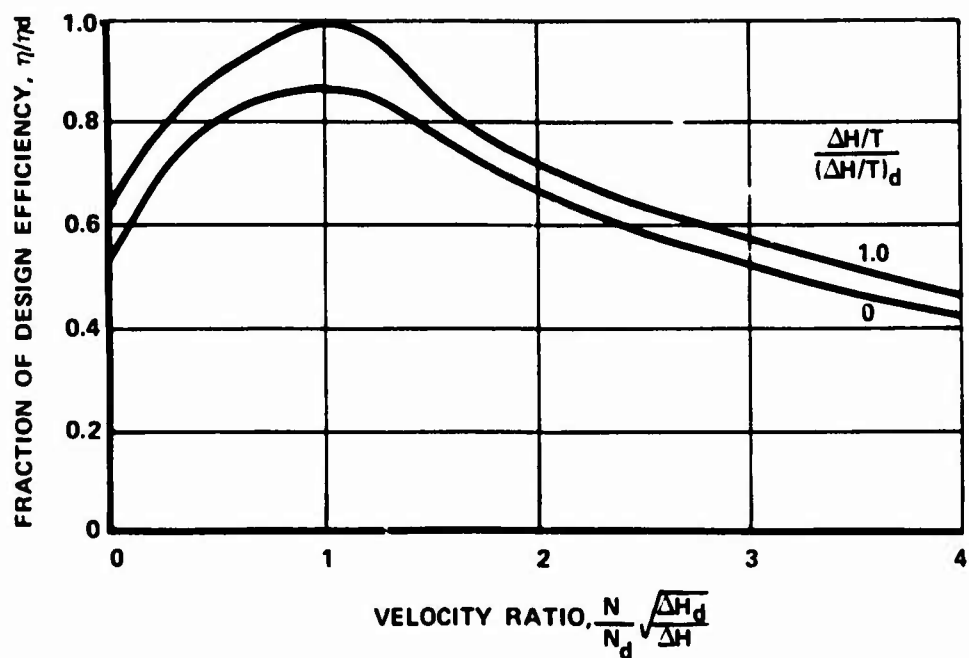
Figure 26. STFRJ368 High Pressure Turbine   FD 73751
Efficiency
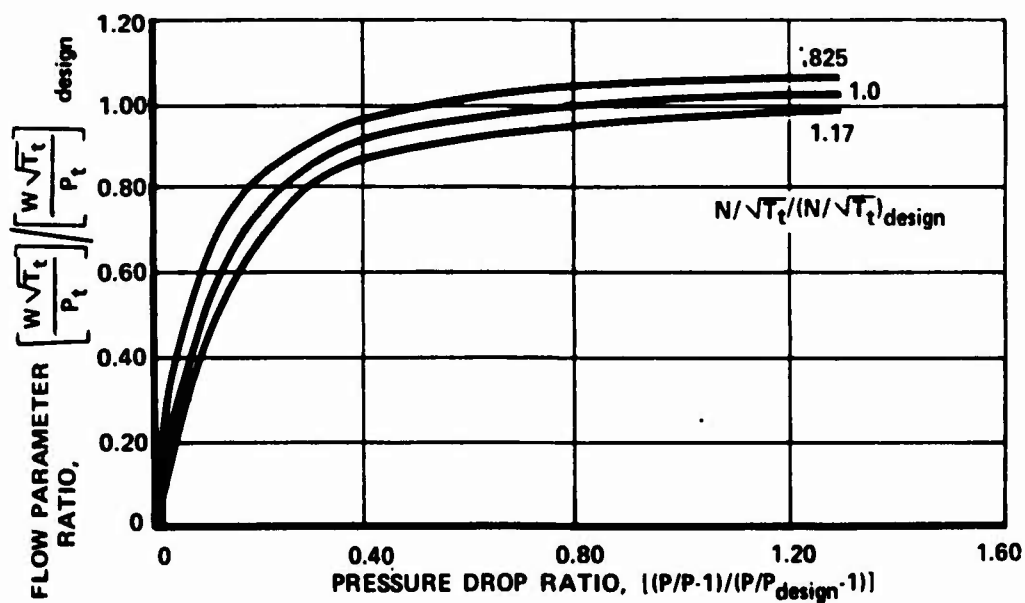
Figure 27. STFRJ368 Low-Pressure Turbine   FD 73752
Flow Parameter vs Pressure Ratio
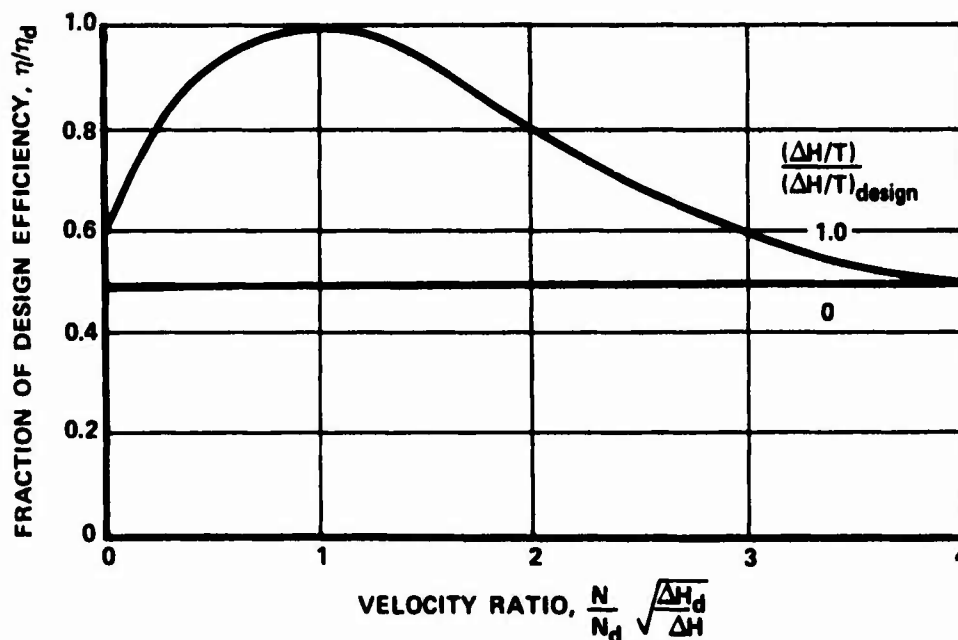
Figure 28. STFRJ368 Low-Pressure Turbine   FD 73753
Efficiency

8.   Duct Nozzle

Exhaust nozzle operation is described by compressible flow relationships.
Inputs to the subroutine are inlet and ambient total pressure and temperature,
nozzle area, and gas flow. Output is required inlet total pressure, or, if not
given, required nozzle area.

9.   Main Engine Nozzle

Operation of the main engine nozzle is the same as for the duct nozzle.

D.   ENGINE DYNAMICS REPRESENTATION

The dynamic relationships between components are described by differential
equations that determine the changes in the independent variables during a transient.
Dynamics are simulated for the two rotor speeds, main burner volume, bypass
duct volume, and engine diffuser volume. Heat transfer dynamics are simulated
by temperature lags on fan discharge, compressor discharge, high turbine inlet,
and fan turbine inlet temperatures. Combustion delays are simulated by tempera-
ture lags on main, fan duct, and ramjet burner temperatures.

1.   Rotor Dynamics

The time rate of change of rotor speed for each rotor is directly proportional
to the difference between the shaft torque generated by the turbine and the shaft
torque absorbed by the compressor. These torques are calculated from the tur-
bine and compressor component thermodynamic and aerodynamic relationships.

37

The steady-state condition that turbine horsepower equal compressor horsepower is modified by the addition of the unbalanced power element ΔHP.

$$HP_{turb} = HP_{comp} + \Delta HP$$

During steady-state iteration ΔHP is zero, whereas during a transient it is calculated as follows:

$$\Delta Q = \frac{(N - N^{n-1})}{\Delta T \cdot CINT}$$

$$CINT = 60/(2\pi \cdot CTVAR)$$

$$\Delta HP = \Delta Q \cdot N/5252$$

where ΔQ - Rotor shaft torque difference, ft-lbf

N - Current rotor speed, rpm

N^{n-1} - Rotor speed at last time, rpm

ΔT - Calculation time increment, sec

$CINT$ - Gain, rpm/ft-lbf-sec

$CTVAR$ - Rotor inertia, ft-lbf-sec^2

5252 - Conversion constant, $(60)(550)/2\pi$, hp-rpm/ft-lbf

2. Pressure-Volume Dynamics

The continuity equation for unsteady flow, the equation of state, and isentropic pressure and temperature relationships describe the gas flow dynamics for a control volume. The engine simulation contains three dynamic control volumes: (1) main burner, (2) a lumped volume including the fan duct, ram duct and combustion duct, and (3) main engine diffuser. The steady-state condition that the flow out of a volume equal the flow into the volume is modified by adding an unbalanced flow element, ΔW:

$$W_{out} = W_{in} + \Delta W$$

During steady-state iteration ΔW is zero whereas during a transient it is calculated by differentiating pressure as a function of time:

$$\Delta W = \frac{(P - P^{n-1})}{\Delta T \cdot CINT}$$

$$CINT = 12 \cdot \gamma \cdot R \cdot T/CTVAR$$

where ΔW – Unbalanced flow, lb_m/sec

   P – Current pressure, psi

   P^{n-1} – Pressure at last time, psi

   ΔT – Calculation time increment, sec

   CINT – Gain, lb_f/lb_m-in.^{2}

   γ – Ratio of specific heats

   R – Gas constant, ft-lb_f/lb_m-°R

   T – Temperature, °R

   CTVAR – Volume, in.^{3}

3.   Temperature Dynamics

The dynamics associated with changes in temperature are caused by transient heat storage effects. When the temperature differential across a component is changed because of a change in the pressure ratio, it is not immediately reflected in the exit temperature of the component. Transient heat storage effects cause the temperature of the airstream to lag the equivalent steady-state value obtained from isentropic temperature ratio and efficiency. This dynamic effect can be described by a first-order differential equation that relates the available temperature change to the actual one. For example, a temperature change at the inlet to a turbine is not immediately reflected in a change in the energy generated by the turbine, because some of the available change in energy goes into heating or cooling the turbine disks and blades. This effect is described by differential equations that relate the change in energy generated by the turbine to the change in energy input to the turbine. Heat storage does not affect the steady-state performance of the system. Heat storage provides temperature dynamic effects that are superimposed upon the basic steady-state gas dynamic equations. Temperature lags are then simulated by the following equation

$$T_\ell = (T_\ell^{n-1}) \cdot e^{-\Delta T/\tau} + T^{n-1}(1 - e^{-\Delta T/\tau}) + (T - T^{n-1})\frac{\tau}{\cdot T} \cdot (e^{-\Delta T/\tau} + \frac{\Delta \Gamma}{\tau} - 1.)$$

where T_ℓ – Lagged value of temperature at current time,

   T_ℓ^{n-1} – Lagged value of temperature at last time, °R

   T – Instantaneous temperature at current time, °R

   T^{n-1} – Instantaneous temperature at last time, °R

   ΔT – Calculation time increment, sec

   τ – Time constant, sec

SECTION VI

SIMULATION OPERATION

A. CONVERGENCE TECHNIQUE

The simulation uses a convergence subroutine termed SMITE* to obtain engine match points. SMITE can determine the values of up to eight independent variables that will minimize an equal number of dependent variables. The dependent variables are calculated as errors between the desired and actual values of engine parameters. The routine is a modified Newton-Raphson convergence technique that calculates the partial derivatives of the dependent variables with respect to each of the independent variables and determines a solution set by iterating on the independent variables until the errors are minimized. SMITE is used in both steady-state and in transient operation. During transients, the independent and dependent variables are changed as the engine operating mode changes.

B. ENGINE SIZING

A useful feature of the program is the ability to scale the size of the engine being simulated. The simulation components have built-in adders and multipliers (scaling factors) and nondimensional maps that allow changing the size of the engine by specifying new design criteria such as fan airflow and pressure ratio, compressor pressure ratio, rotor speeds, burner temperature, etc. A size point with the desired design criteria is run before every case to set the internal component scaling factors and flow areas.

C. ENGINE OPERATING MODES

The simulation mode of operation is determined by the position of the ram duct doors, fan duct doors, and main engine nozzle. The position of these control variables and the resulting mode of operation is shown in table V.

Table V. Engine Operating Modes

	Engine Mode	Ram Duct Doors	Fan Duct Doors	Main Engine Nozzle
1.	Turbofan	Closed	Open	Open
2.	Dual	Open	Open	Open
3.	Fan Duct-Ramjet	Open	Open	Closed
4.	Turbojet-Ramjet	Open	Closed	Open
5.	Ramjet	Open	Closed	Closed

---

*McNeill, D. K., and J. L. Forgham, Fast Stable Convergence for Gas Turbine Computer Simulations PWA FR-3145, 19 March 1969.

1.   Turbofan Mode

In the following descriptions of modes of operation it is assumed that the given flight condition sets engine inlet and ambient conditions, hence those pressures and temperatures will not be considered as independent variables. In turbofan mode a match point is determined by specifying the fan and compressor operating points and main burner temperature. The only constraints are the two turbine flow parameters. Since the fan and compressor operating points are determined by specifying rotor speeds and M-line (pressure ratio divided by corrected airflow) five independent variables are to be determined. The two turbine flow parameters result in two dependent variables; the errors between actual and calculated flow parameters. Three independent variables must be given and the other two can be determined by SMITE. Additional dependent variables can be added by specifying additional constraints. For example, specifying a desired fan airflow will result in a dependent variable calculated as the error between actual and desired fan airflow. Typically, in turbofan mode, fan airflow, fan M-line, and main burner temperature are given. SMITE then calculates values for fan speed, compressor speed, and compressor M-line.

2.   Dual Mode

In addition to the turbofan mode constraints, in the dual mode there is the added constraint that at the fan/ram duct mixing plane the fan duct and ramjet duct static pressures must be equal. The error between these two pressures provides an additional dependent variable. Additional independent variables are ramjet inlet airflow, fan duct burner temperature, and ramjet burner temperature. If the fan duct burner and ramjet burner temperatures are given or calculated from given fuel flows, a dual mode matchpoint can be obtained by adding ramjet inlet airflow and the static pressure error to the turbofan mode SMITE matrix.

3.   Fan Duct-Ramjet Mode

In the fan duct-ramjet mode there are no turbofan constraints. The only dependent variable is the static pressure error. The independent variables are ramjet inlet airflow, fan inlet airflow, fan duct burner temperature, and ramjet burner temperature. Typically, an additional dependent variable is generated by specifying a duct nozzle area and calculating the error between actual and desired nozzle pressure. If fan duct and ramjet burner temperatures are known, SMITE can determine the values of ramjet and fan inlet airflows.

4.   Turbojet-Ramjet Mode

Operation in the turbojet-ramjet mode is the same as in the dual mode with the absence of the static pressure balance constraint. In its place is the constraint that fan airflow must equal compressor airflow. The dependent variable calculated as the static pressure error becomes the error between fan and compressor airflow. This mode of operation occurs only at very low fan rotor speeds usually near the end of a turbofan to ramjet transition, and is little used.

5.   Ramjet Mode

In the ramjet mode there are two independent variables, ramjet inlet air-
flow and burner temperature. Since there are no constraints, no iteration is
required if both independent variables are specified. Iteration is required if
constraints are added. For example, during transients, duct nozzle area and
ramjet burner fuel flow are given. SMITE is then used to determine ramjet inlet
flow to minimize the dependent variable calculated as the error between actual
and required nozzle pressure which is a result of the given nozzle area.

SECTION VII

TRANSIENT OPERATION

A.   ENGINE CONTROL VARIABLES

The engine control variables used to simulate a transient are main engine burner fuel flow, fan duct burner fuel flow, ramjet burner fuel flow, main engine nozzle area, duct nozzle area, fan duct door area, ramjet duct door area. (See figure 29.) In the simulation, the fuel flows can be either specified directly or can be calculated by specifying burner temperature or fuel-air ratio.
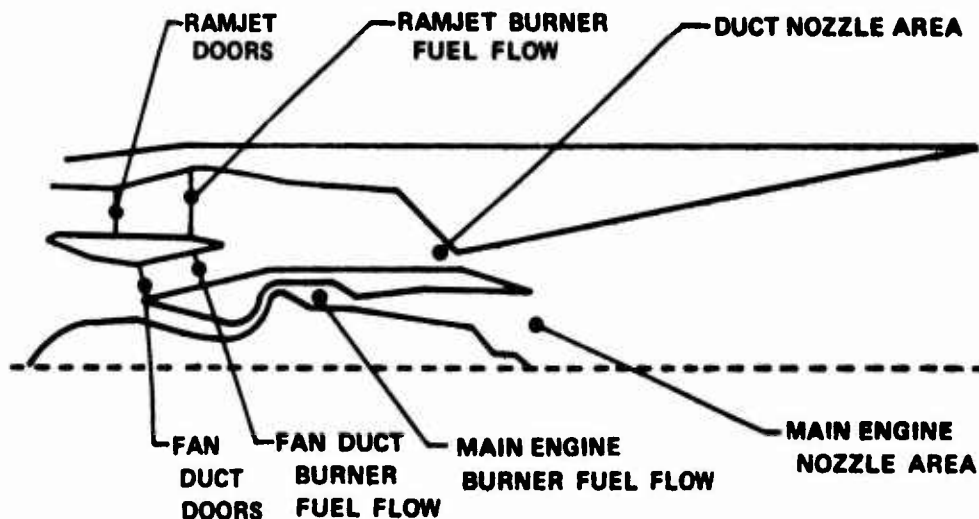
Figure 29. STFRJ368 Engine Control Variables   FD 73754

Since the simulation does not yet include a control system, the values of the control variables during a transient must be specified by the user as functions of time or some other engine parameter. It is also possible to let SMITE predict the value of a control variable to satisfy some added constraint. For example, SMITE could calculate the duct nozzle area during a transient to maintain a constant total engine airflow.

B.   TRANSIENT OPERATION

Beginning at time = 0, the simulation advances time by a calculation time increment ΔT. At each time step SMITE iterates for values of the independent variables to satisfy the given constraints. User input changes in control variables result in changes in the dependent variables, which in turn cause SMITE to iterate to obtain a new solution set of independent variables. The rate of change of the independent variables from one time step to the next is regulated by the unbalanced dynamic elements previously described. The process continues for any desired length of simulation time, thus describing engine transient performance as a series of discrete engine matchpoints.

43

SECTION VIII

TRANSIENT TRANSITION TEST CASES

A. TURBOFAN TO RAMJET

Transient test cases have been run to verify the capability of the program's logic to simulate engine transitions. The following is a description of a transition from turbofan to ramjet. Figures 30a through 30e show plots of various engine parameters as functions of time plotted with the simulation's graphic routines.

The selected flight condition is Mach 2.5, 37,000 ft. At the start of the transition, the engine is in turbofan mode at a power setting producing 48,200 lb_f net thrust and 190 lb_m/sec fan inlet corrected airflow. The total aircraft inlet airflow is 250 lb_m/sec and will be held constant during the transition. It is assumed that until the ramjet doors are fully open the aircraft inlet bypass doors are open to bypass the excess airflow. When the ramjet doors are fully open the inlet bypass doors are assumed to be fully closed and the duct nozzle controls total engine airflow to the desired value of 250 lb_m/sec. The fan duct burner is run to fuel-air ratio input as a function of time. The ramjet burner is also run to fuel-air ratio input as a function of time but with a closed loop trim to hold total net thrust near the desired level. The main engine burner is run to fuel flow input as a function of time. The main engine nozzle area is scheduled as a function of time. The duct nozzle area is scheduled as a function of time until the ramjet doors are fully open, then it is varied by SMITE to hold constant engine airflow. The fan duct and ramjet duct doors are scheduled as functions of time.

The transition begins in turbofan mode by opening the duct nozzle area to lower the duct static pressure. At 0.6 sec the duct static pressure is lower than the engine inlet total pressure and the ramjet doors begin to open. As the ramjet doors open ramjet airflow increases. At 1.0 sec the ramjet burner is lit, the thrust control trim action begins, and fan duct burner fuel air ratio is lowered slightly. The simulation is now in dual mode. At 1.6 sec the ramjet doors are fully open and the duct nozzle begins to control total engine airflow. From 1.5 to 2.2 sec the main engine burner fuel flow is reduced to minimum to decelerate the turbofan. The turbofan continues to decelerate until 7.5 sec. During this time, the main engine nozzle area is reduced, the ramjet burner fuel-air ratio is trimmed to hold thrust, and the duct nozzle area is varied to hold constant engine airflow. At 7.52 sec the main engine burner is shut off and the turbofan begins to windmill. Since the program cannot simulate windmill operation the turbofan calculations are bypassed for the remainder of the transition. This assumption is justified because, with the main engine burner shut off and the fan at a pressure ratio near 1.0, turbofan performance is no longer critical and can therefore be neglected.

Also at 7.5 sec the fan duct doors begin to close. At 8.0 sec the fan duct burner is shut off, the fan duct doors are fully closed, and the engine is in ramjet mode, completing the transition. Since the main engine nozzle is not fully closed, there is a small amount of airflow passing through the core engine, which is assumed to be windmilling.

44
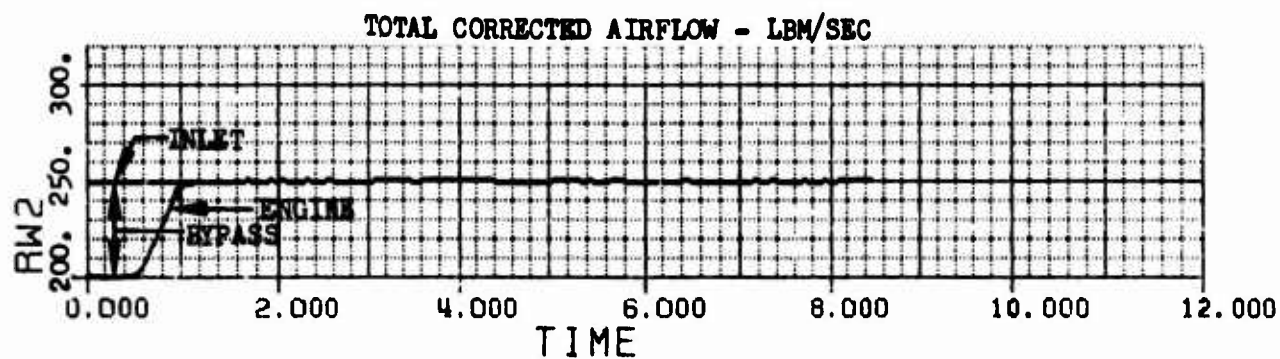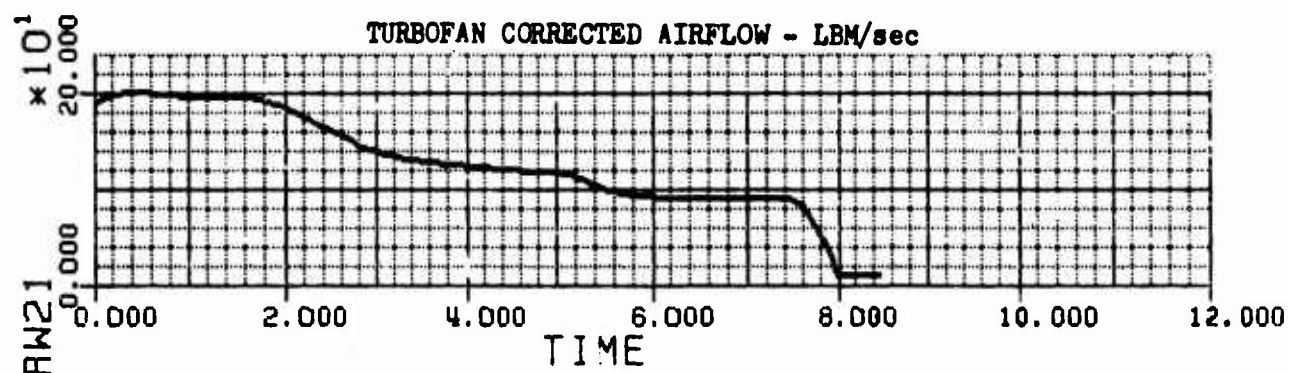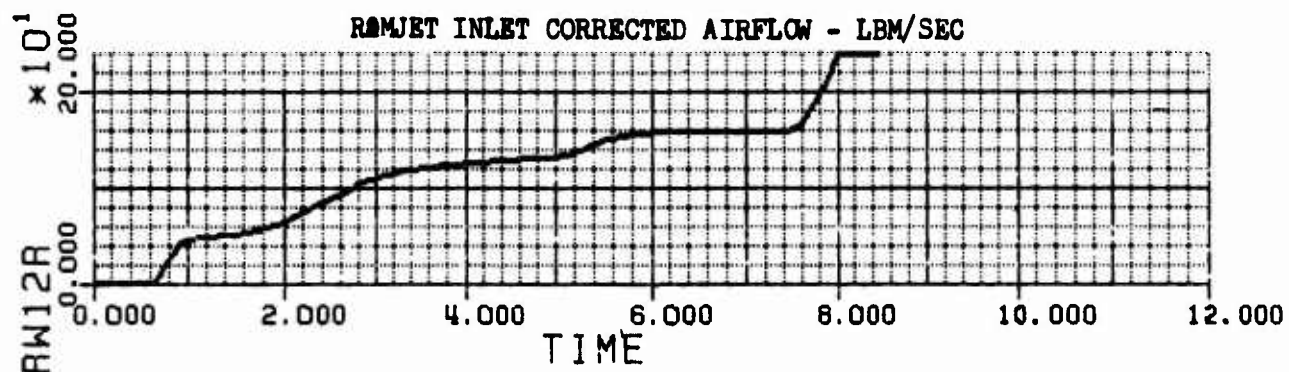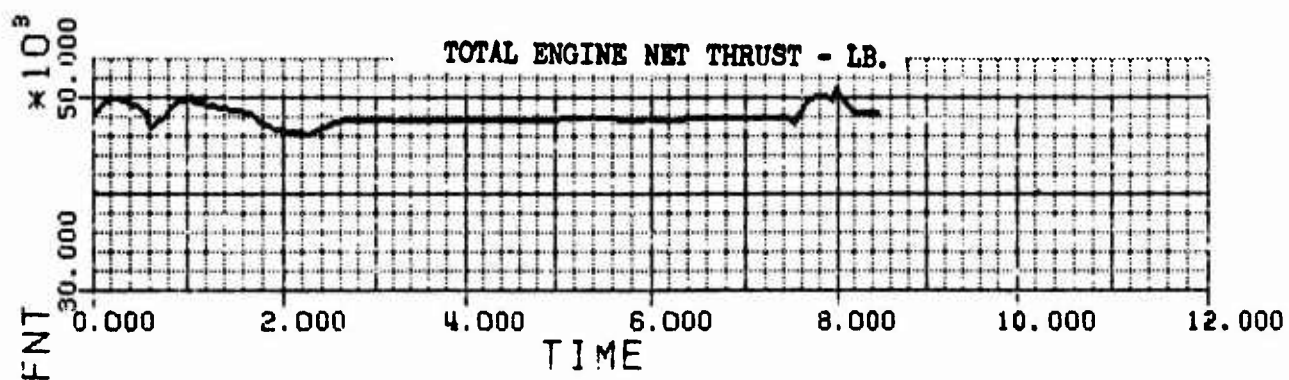
Figure 30a. STFRJ368 Turbofan Ramjet 37K ft
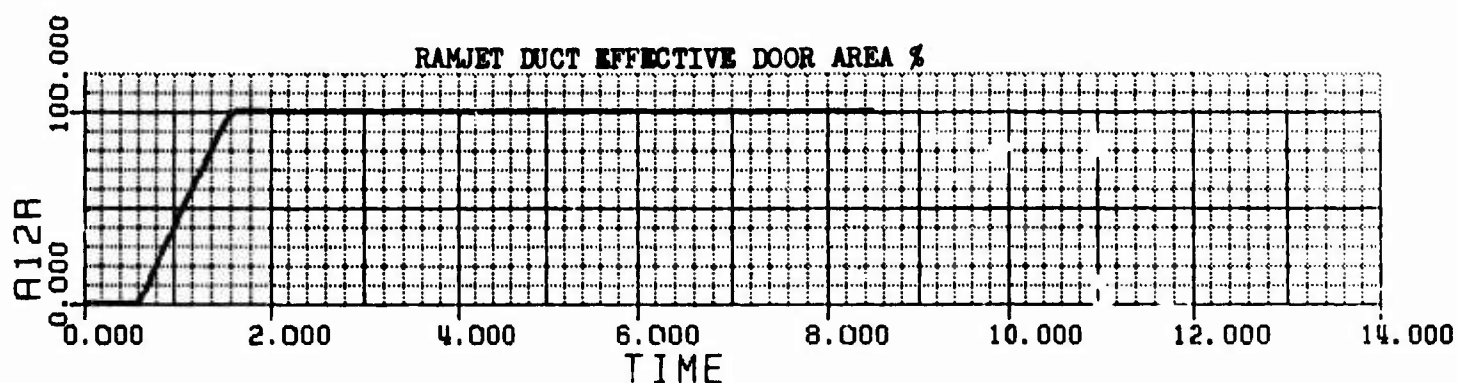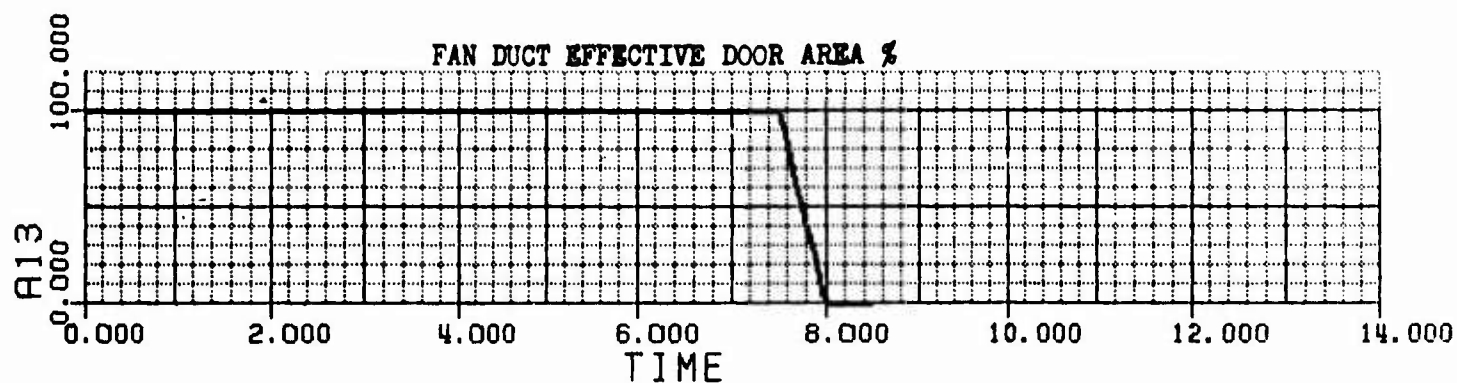Mach 2.5 Transition Turbofan to
Ramjet

45
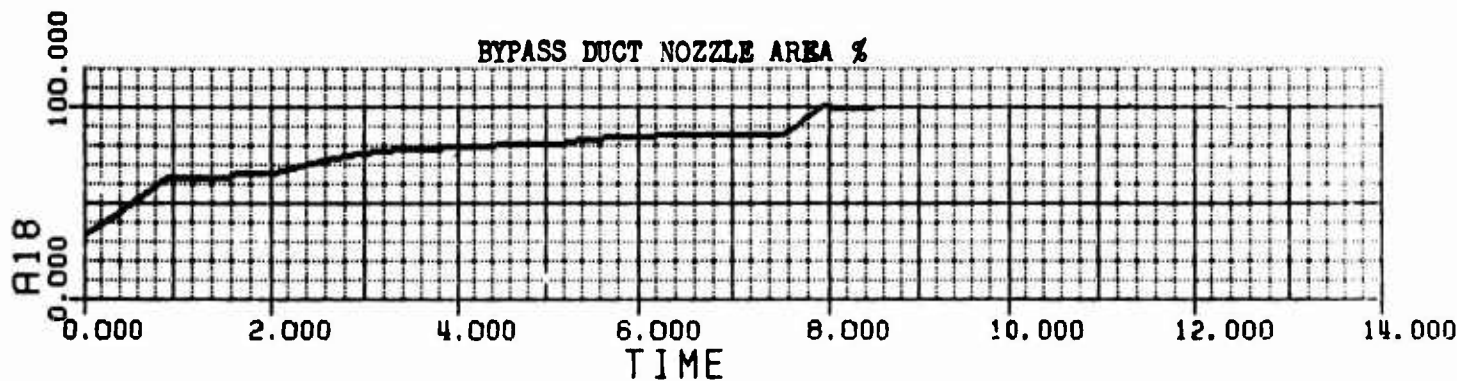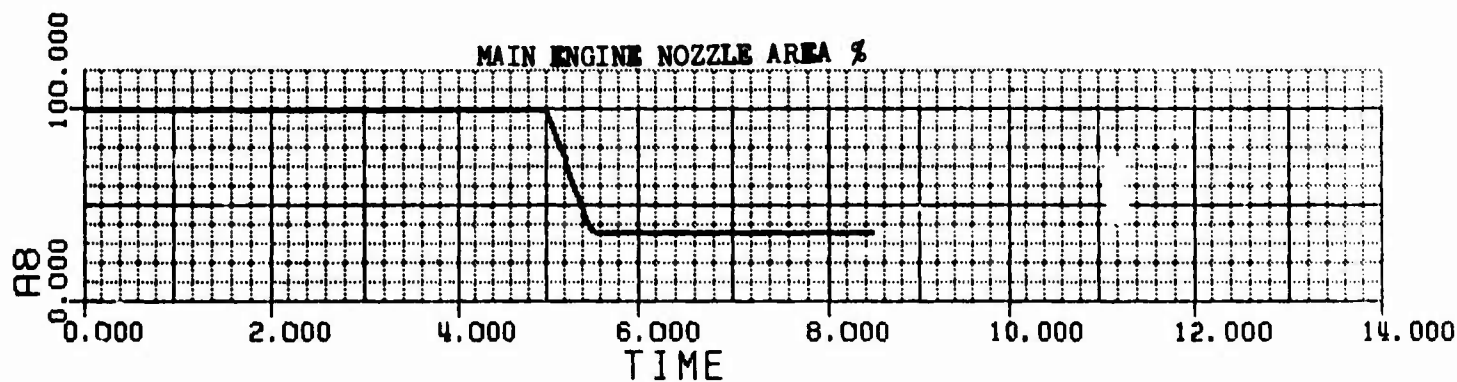
Figure 30b. STFRJ368 Turbofan Ramjet 37K ft
Mach 2.5 Transition Turbofan to
Ramjet (Continued)

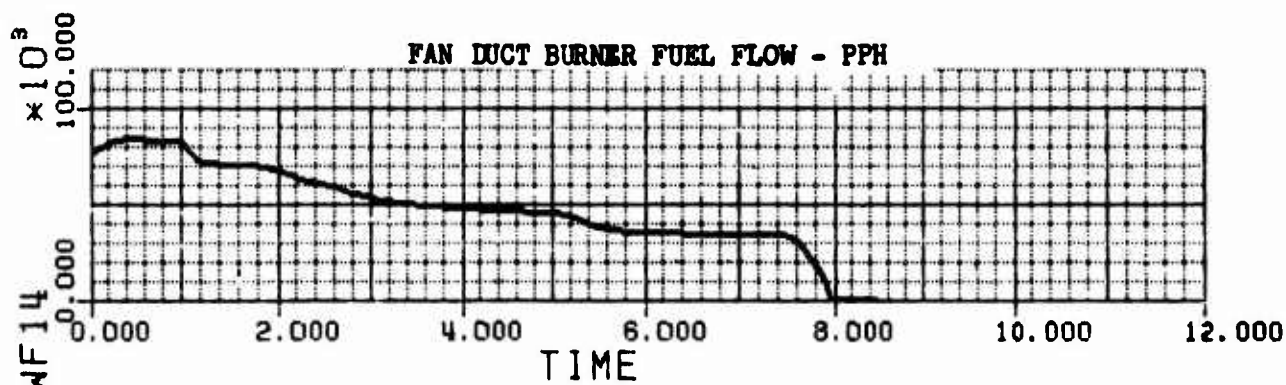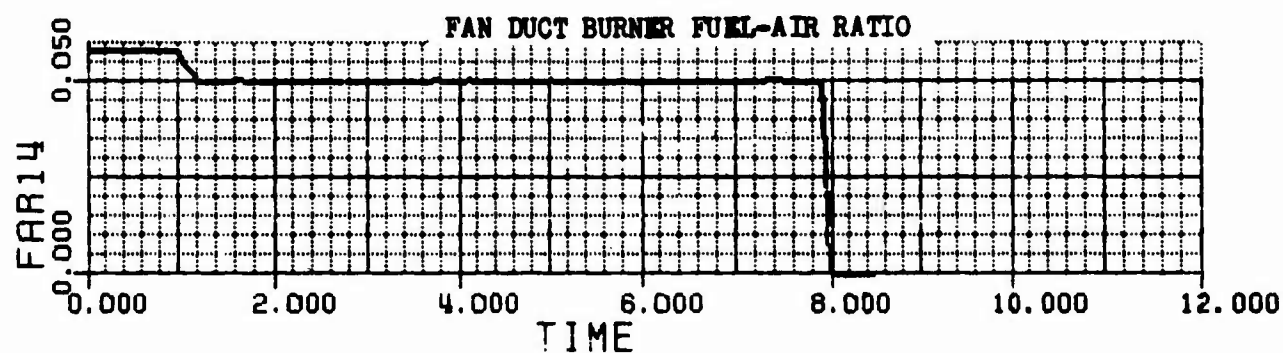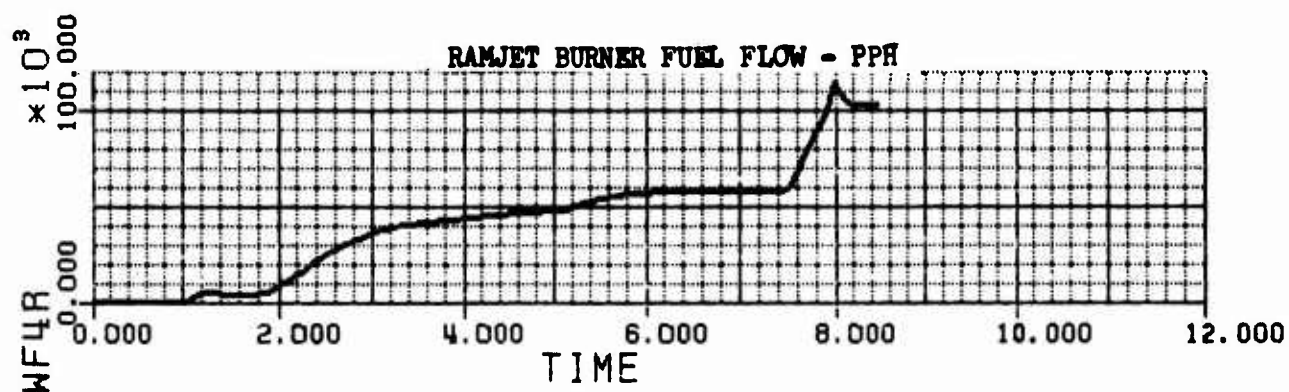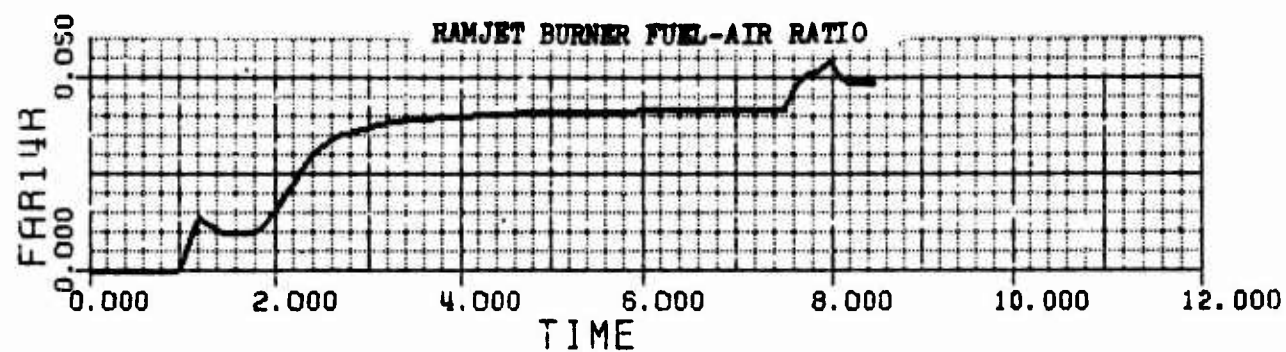Figure 30c. STFRJ368 Turbofan Ramjet 37K ft
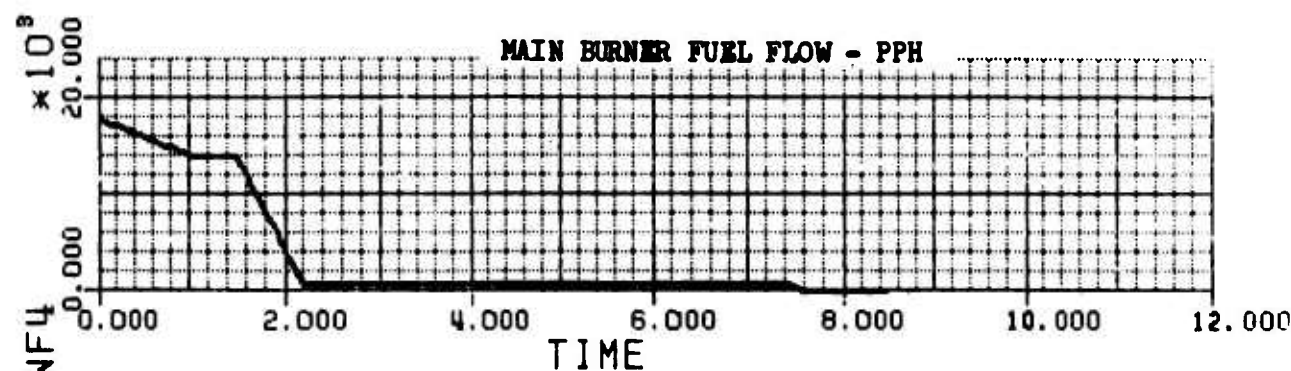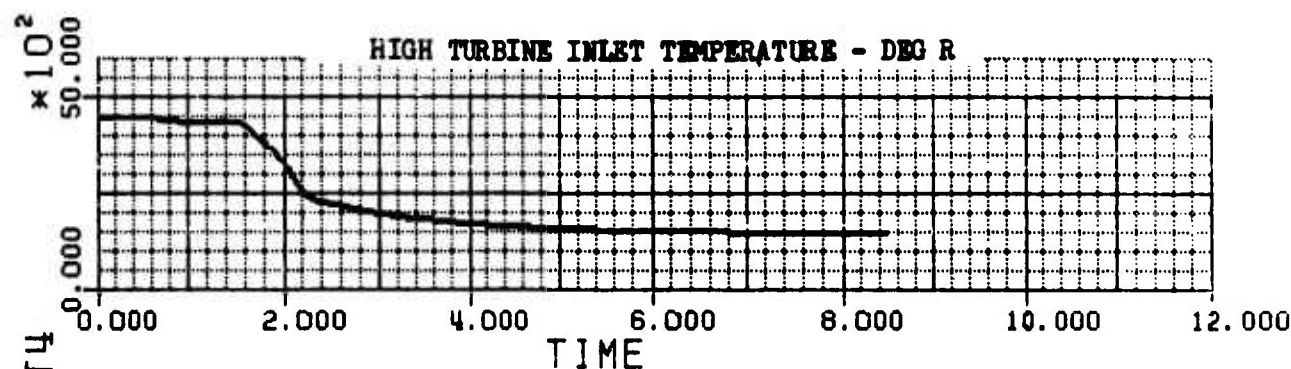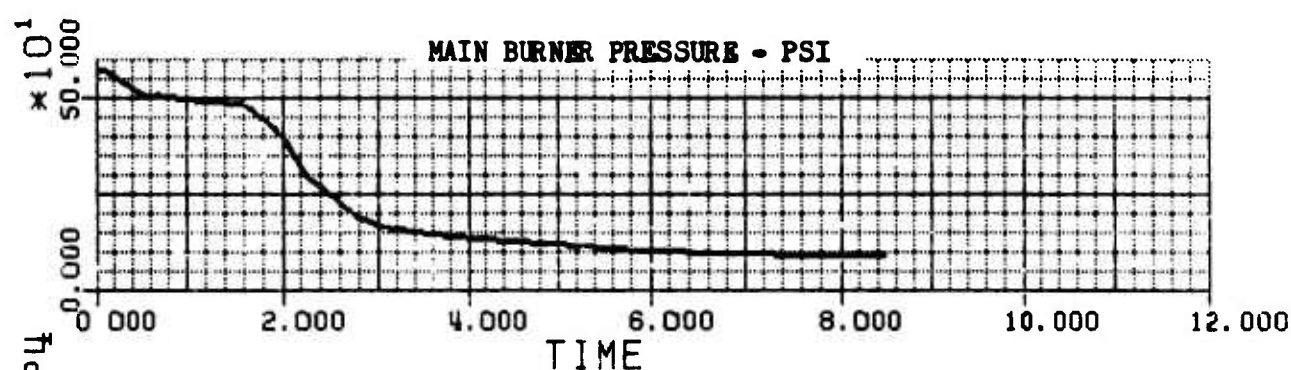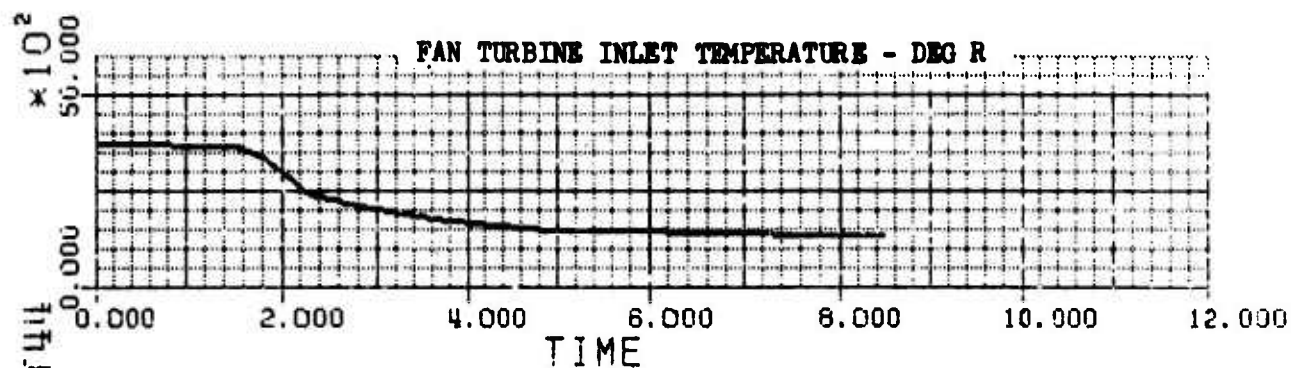Mach 2.5 Transition Turbofan to
Ramjet (Continued)

Figure 30d. STFRJ368 Turbofan Ramjet 37K ft
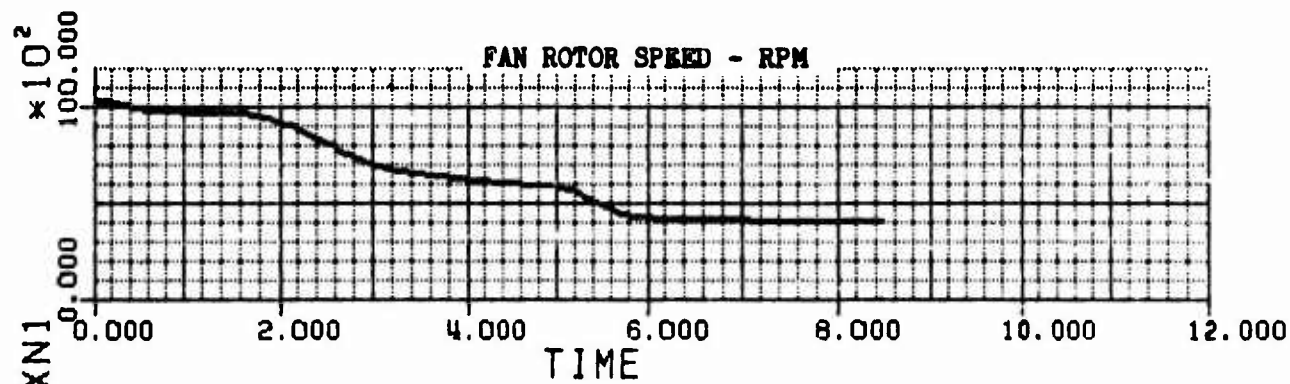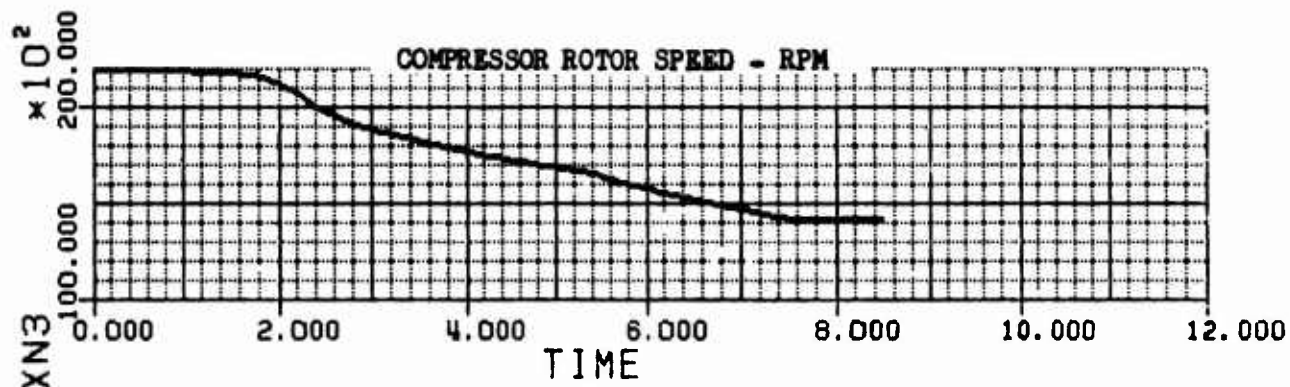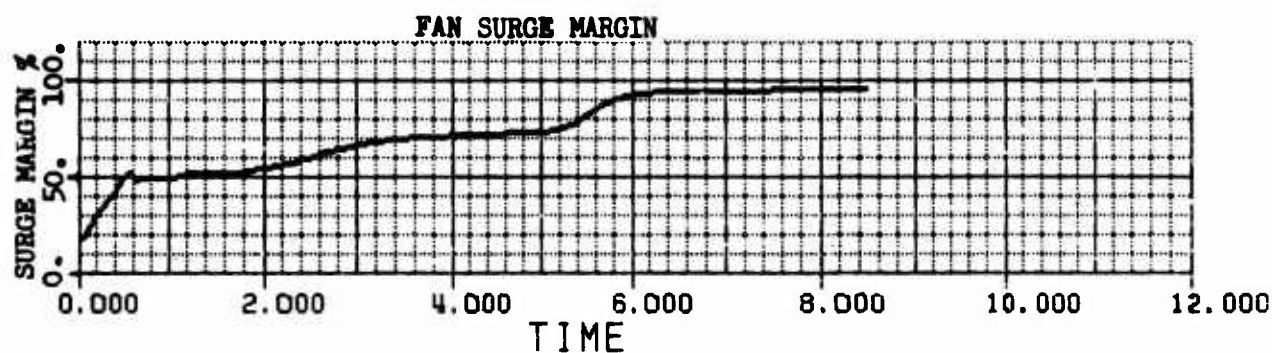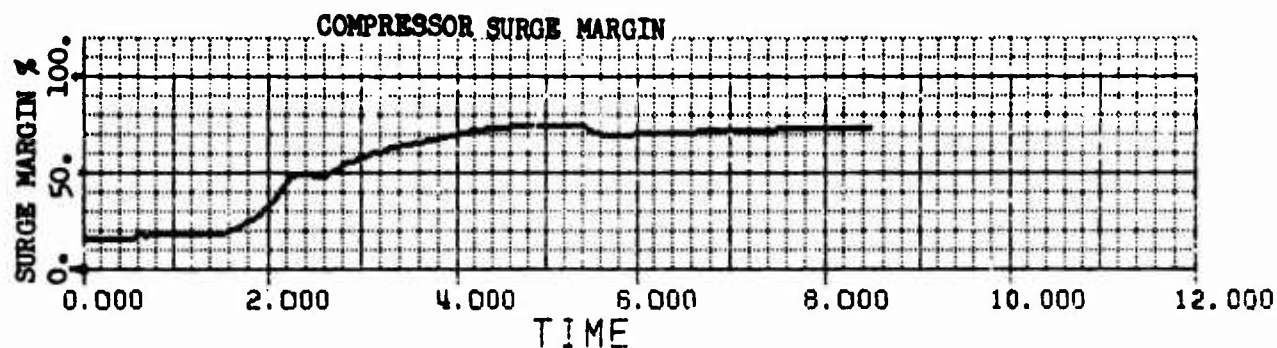Mach 2.5 Transition Turbofan to
Ramjet (Continued)

48

Figure 30e. STFRJ368 Turbofan Ramjet 37K ft
Mach 2.5 Transition Turbofan to
Ramjet (Continued)

As shown in figure 30a, this test transition was accomplished with a gradual ramp in airflow between the selected turbofan and ramjet levels, and nearly constant thrust (about ±6% variation). It thus appears that the turbofan-to-ramjet transition can be accomplished without unexpected problems. Control studies to be conducted in Phase II will be concentrated on the control logic needed to perform transition within the limits of a realistic control system.

B. RAMJET TO TURBOFAN

A transition from ramjet to turbofan, illustrated in figures 31a through 31e, was run as follows. Again the flight condition is Mach 2.5, 37,000 ft. The duct nozzle is used to hold constant engine airflow until the ramjet doors begin to close. At that time it is assumed that the inlet bypass doors would begin to open and bypass the excess airflow. The performance of the turbofan is neglected until the main engine burner is ignited. At that time it is assumed that the turbofan would be at an operating point reached by windmilling. The ramjet and fan duct burners are run to fuel-air ratio scheduled as functions of time with closed loop trimmers to control total net thrust. The main engine burner is run to fuel flow scheduled as a function of time. The fan duct doors, ramjet doors, and main engine nozzle areas are scheduled as functions of time. The duct nozzle area is set by SMITE to hold constant engine airflow until the ramjet doors begin to close, then it is scheduled as a function of time.

The transition begins with the engine in ramjet mode at the desired thrust level. To initiate the transition, the fan duct doors are opened between 0.2 and 1.2 sec. During this time the engine is in fan duct - ramjet mode. At 1.2 sec the main engine burner is ignited at minimum fuel flow. The engine is now in dual mode and turbofan performance begins to be calculated. The ramjet burner fuel-air ratio is continuously being trimmed to hold thrust. However, at 1.0 sec the maximum allowable fuel-air ratio is reached and thrust momentarily falls off until the fan duct burner is ignited at 1.5 sec. At this point the fan duct burner fuel-air ratio also begins to be trimmed to control thrust. The trim action on the ramjet and fan duct burner fuel-air ratio brings thrust to the desired level by 1.8 sec. Meanwhile the main engine nozzle area is increased between 1.2 to 2.0 sec and main engine burner fuel flow is increased to accelerate the turbofan.

At 6.4 sec the ramjet burner fuel-air ratio is decreased and at 6.6 sec the ramjet doors begin to close. Thrust begins to fall off and the fan duct burner fuel-air ratio is trimmed up to hold thrust. At 7.2 sec the ramjet burner is shut off and the ramjet doors are fully closed. Although the fan duct burner fuel-air ratio is trimmed to the maximum, thrust falls off since the turbofan has not yet accelerated to full power. The final thrust loss could be prevented by waiting until the turbofan is at full power before shutting off the ramjet. A control system (which is to be incorporated into the simulation in Phase II) is required for faster turbofan acceleration without compressor and fan stall.

The transition from ramjet to turbofan thus appears to be more difficult than from turbofan to ramjet, from the standpoint of thrust variations. Inlet airflow was held constant, however, so that inlet stability should not be a problem. The control system studies to be conducted in Phase II will include an effort aimed at reducing thrust variations during this transition.
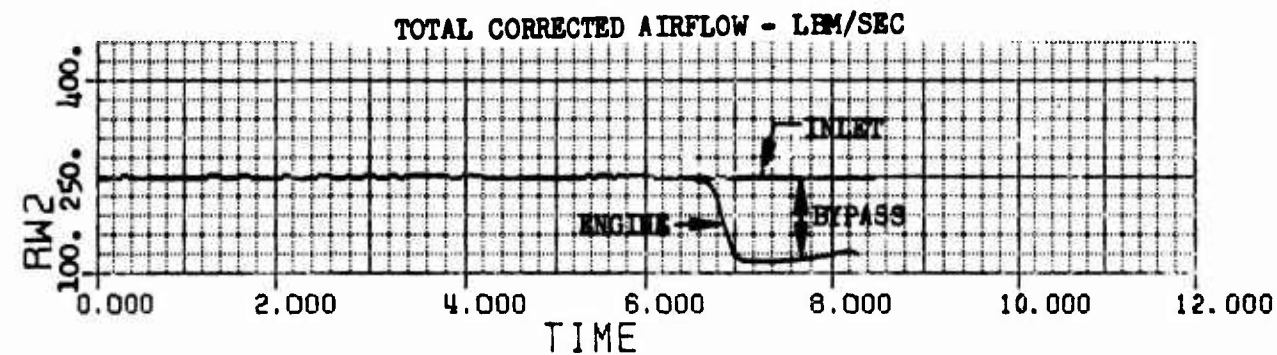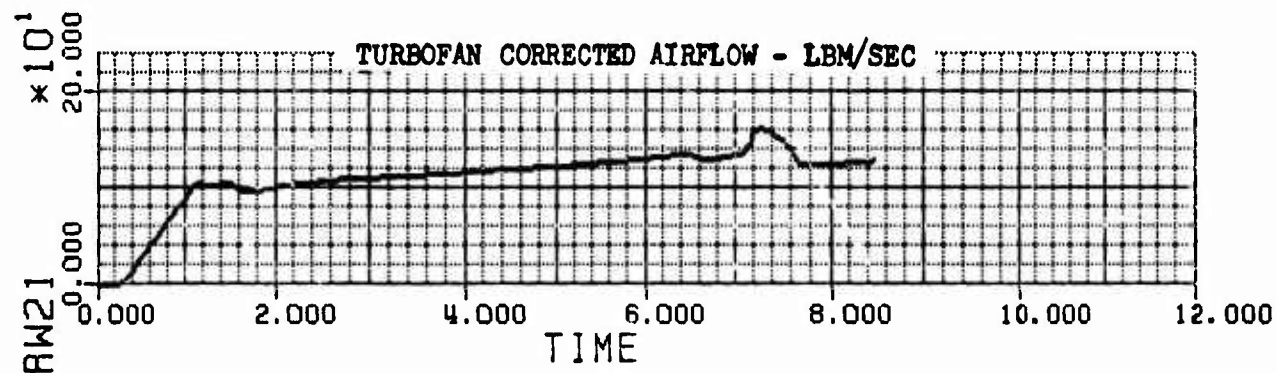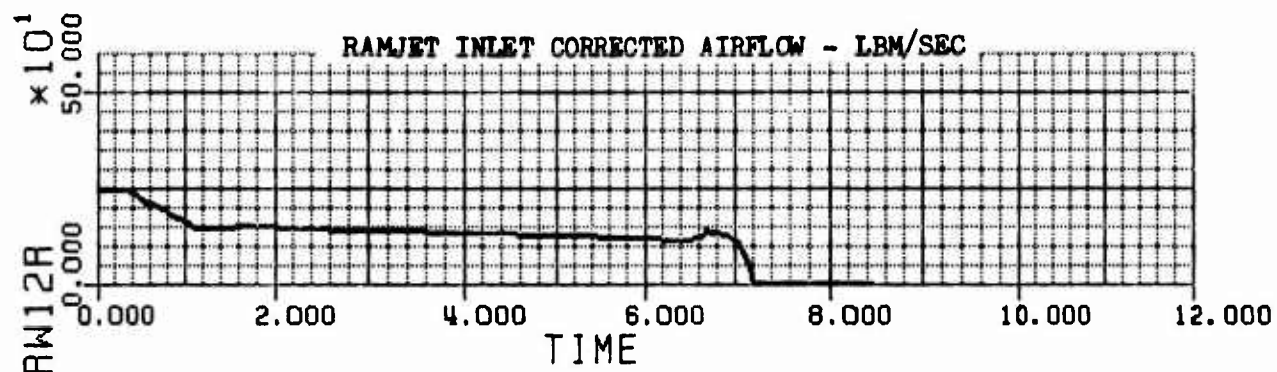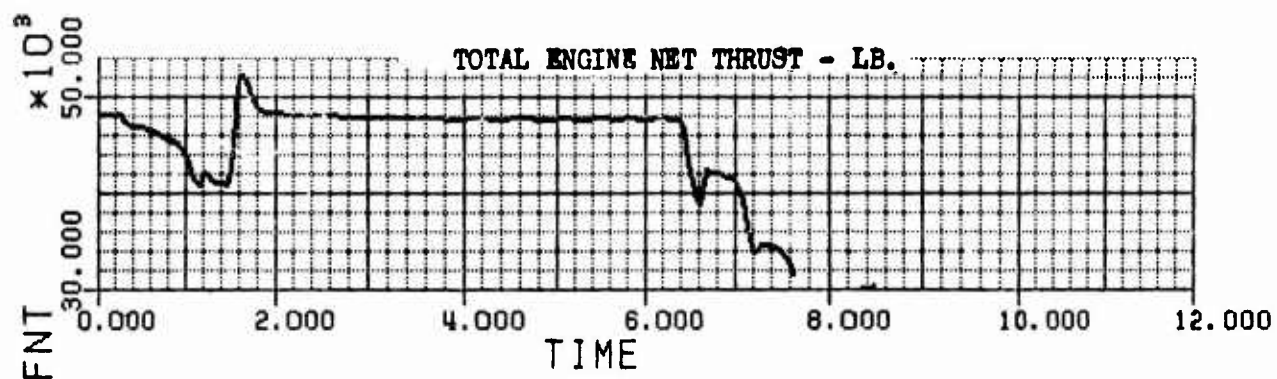
Figure 31a. STFRJ368 Turbofan Ramjet 37K ft
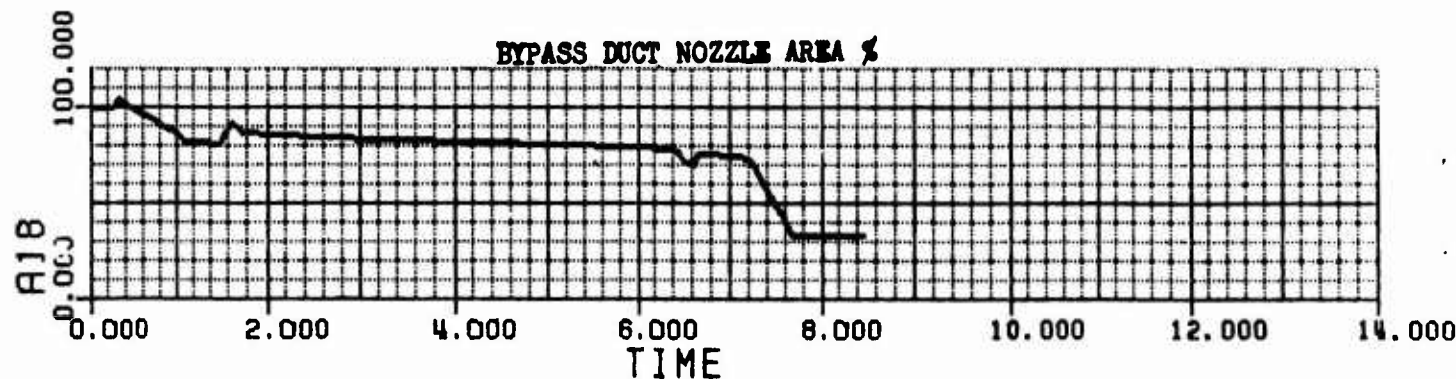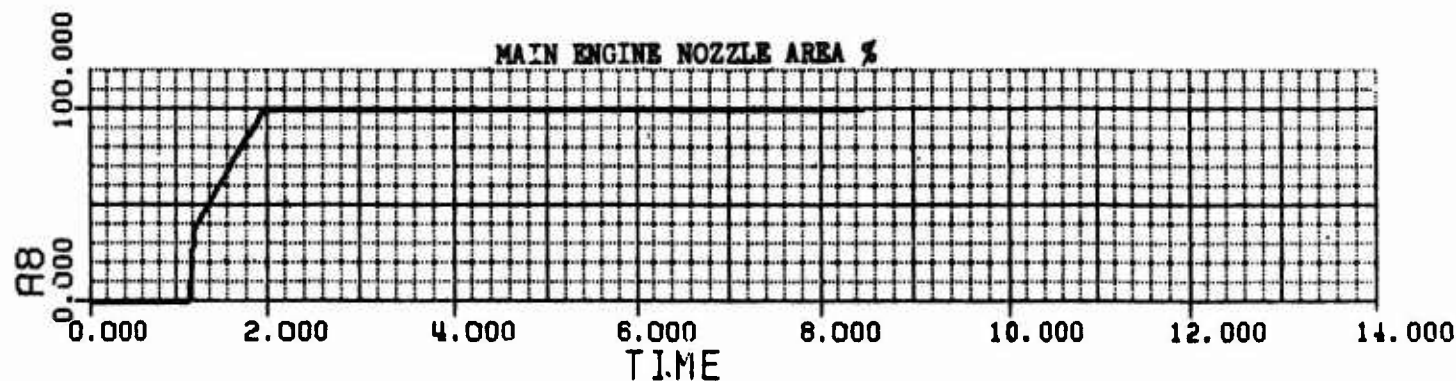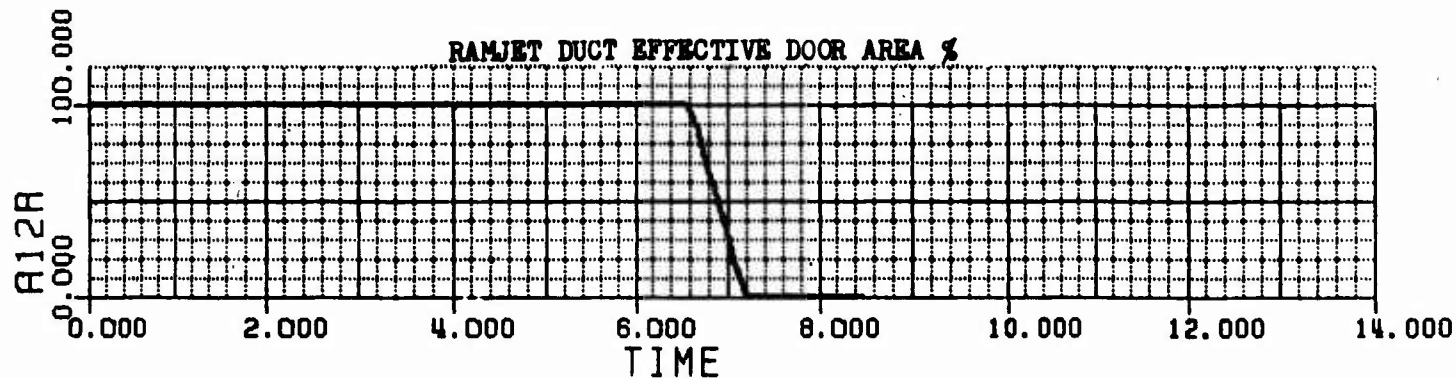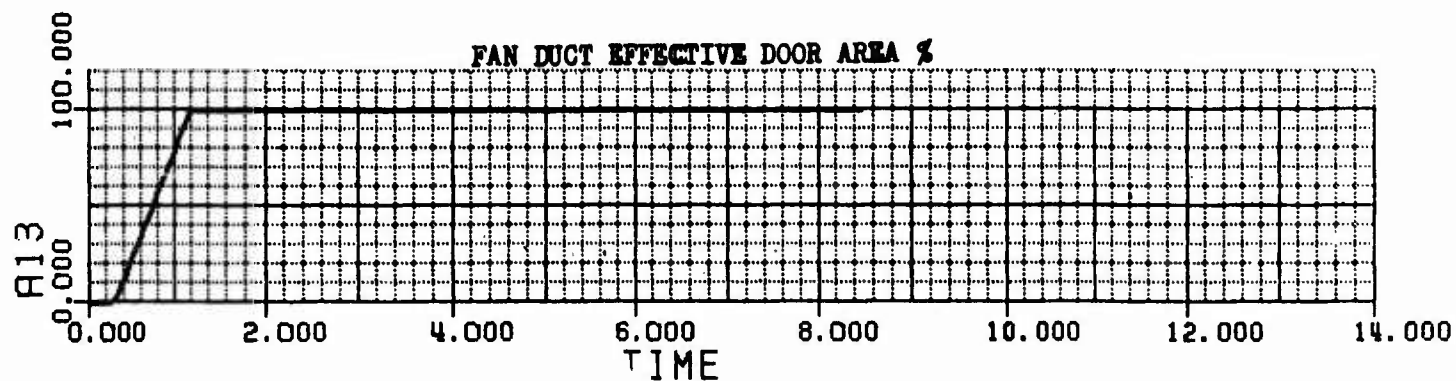Mach 2.5 Transition from Ramjet
to Turbofan

51

Figure 31b. STFRJ368 Turbofan Ramjet 37K ft
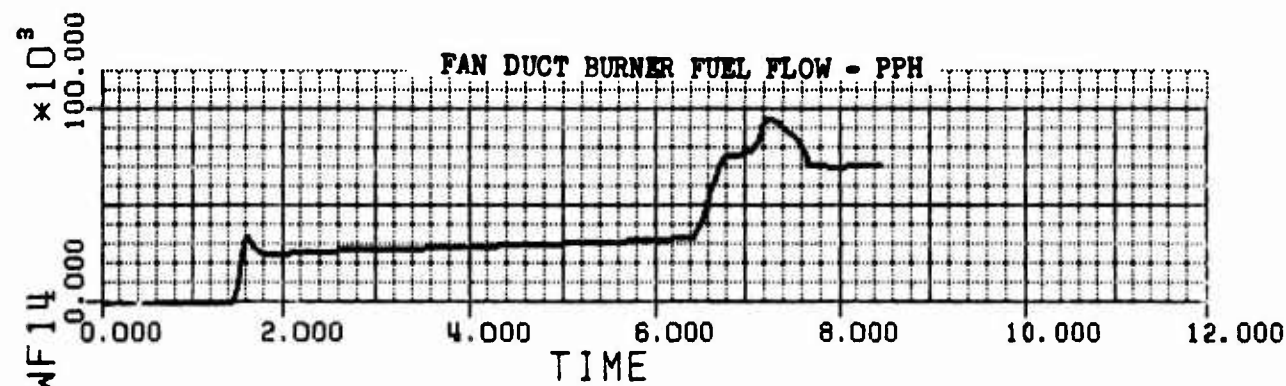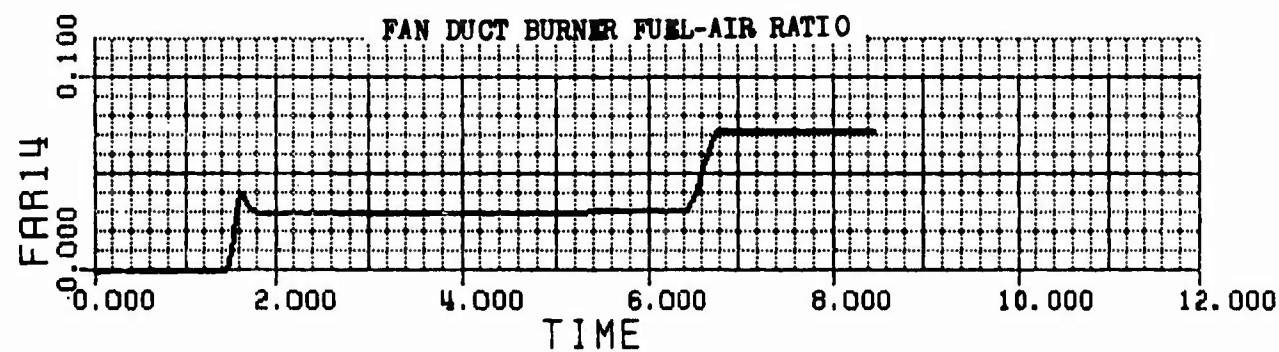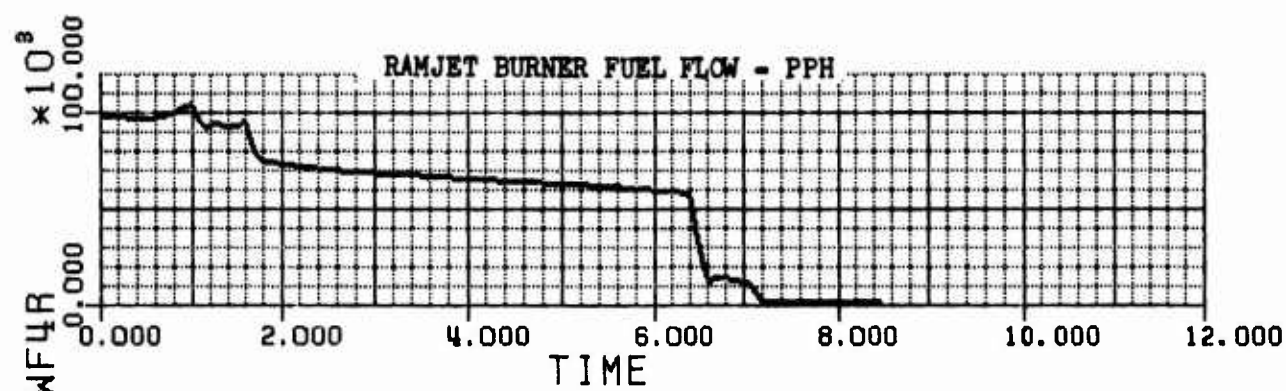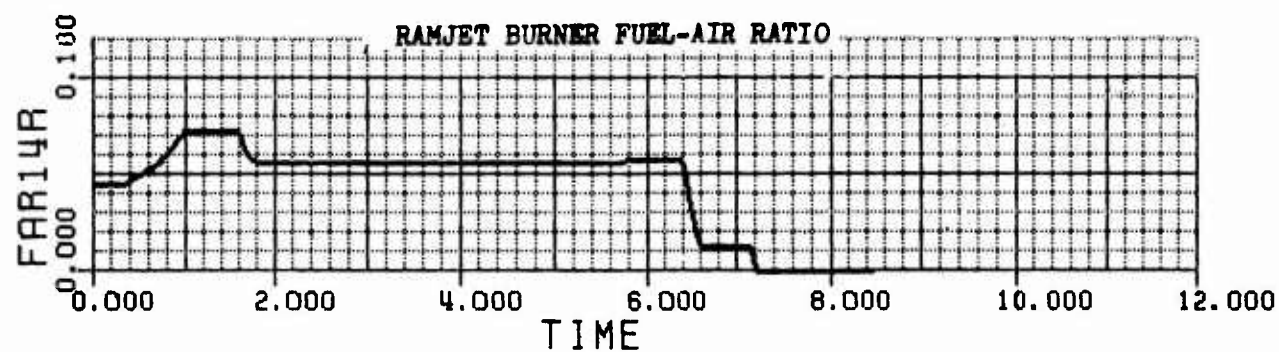Mach 2.5 Transition Ramjet to
Turbofan (Continued)

Figure 31c. STFRJ368 Turbofan Ramjet 37K ft
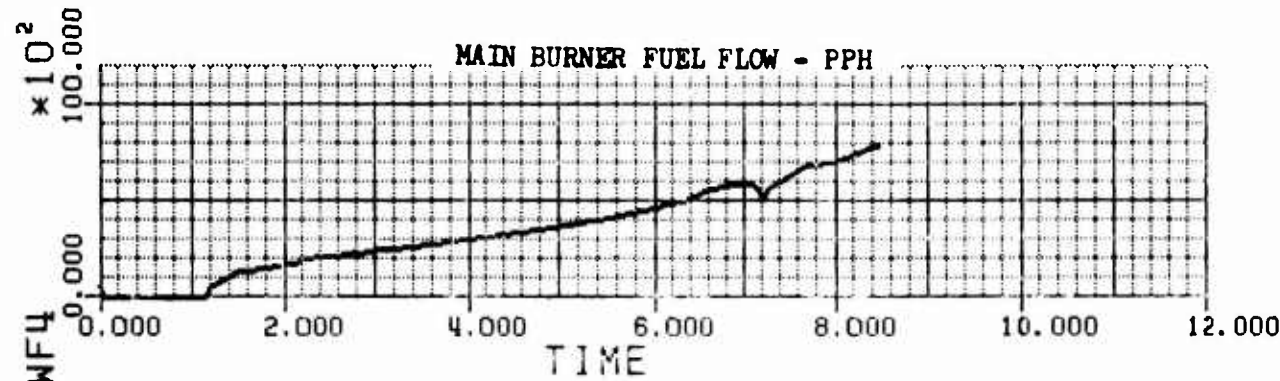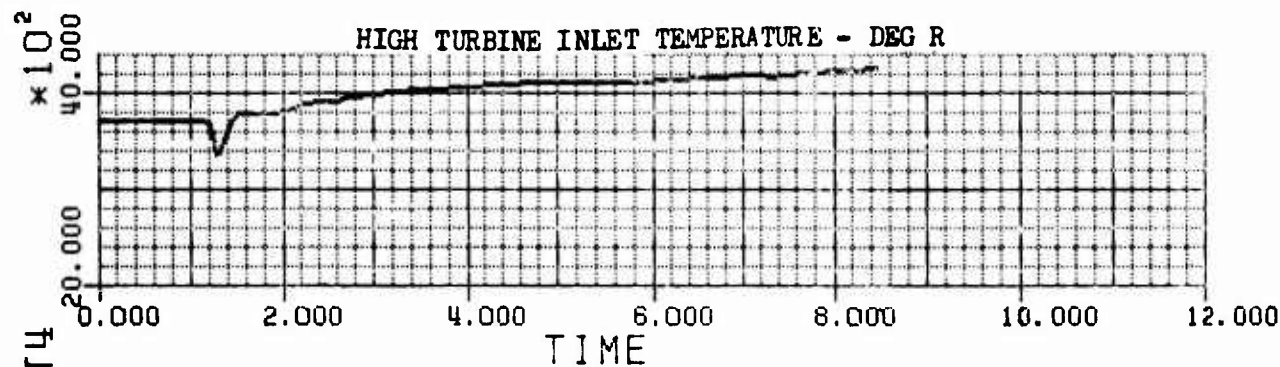Mach 2.5 Transition from Ramjet
to Turbofan (Continued)

Figure 31d. STFRJ368 Turbofan Ramjet 37K ft
Mach 2.5 Transition from Ramjet
to Turbofan (Continued)

54
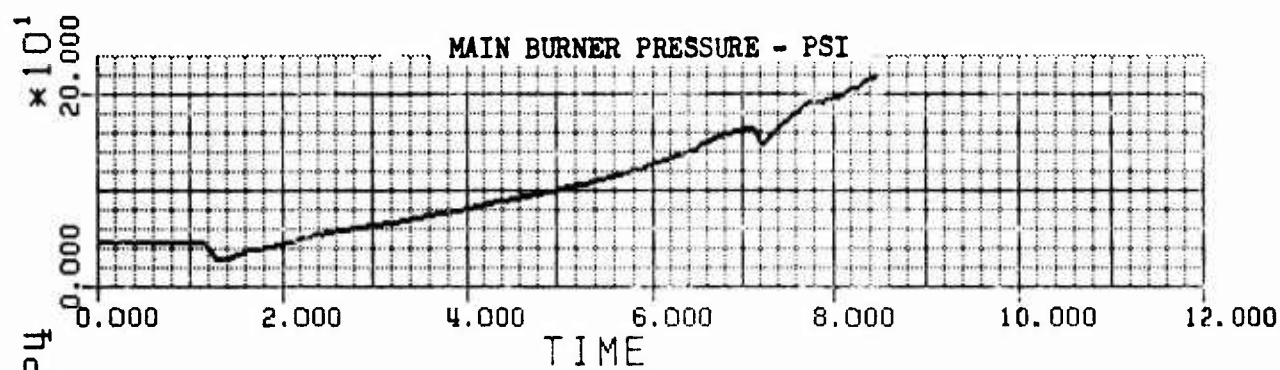
Figure 31e. STFRJ368 Turbofan Ramjet 37K ft
Mach 2.5 Transition from Ramjet
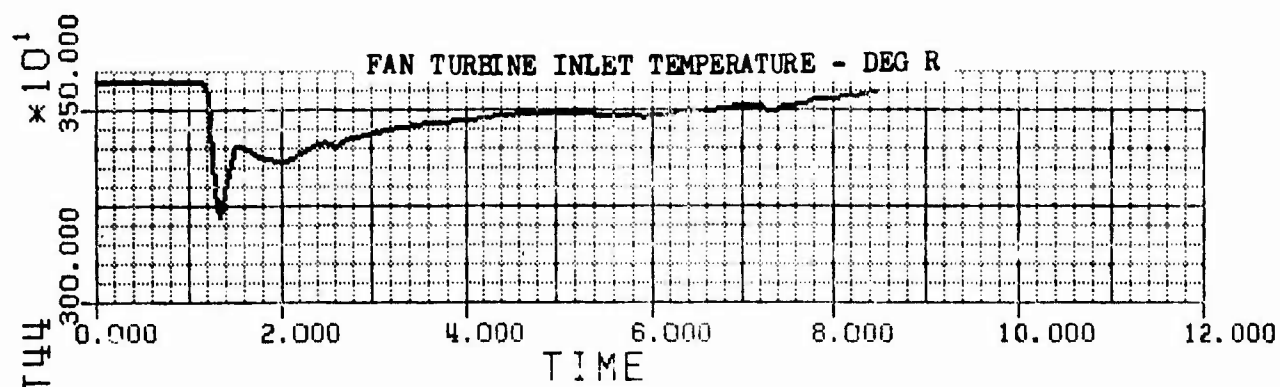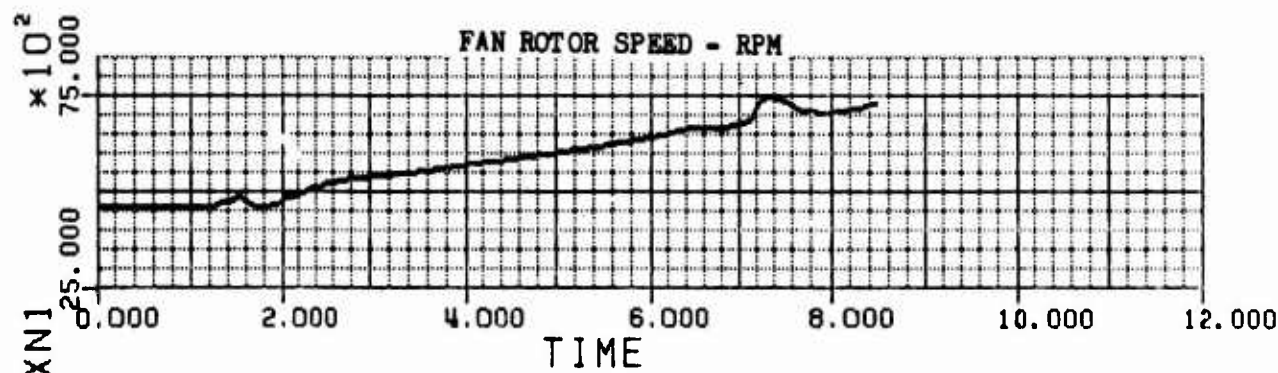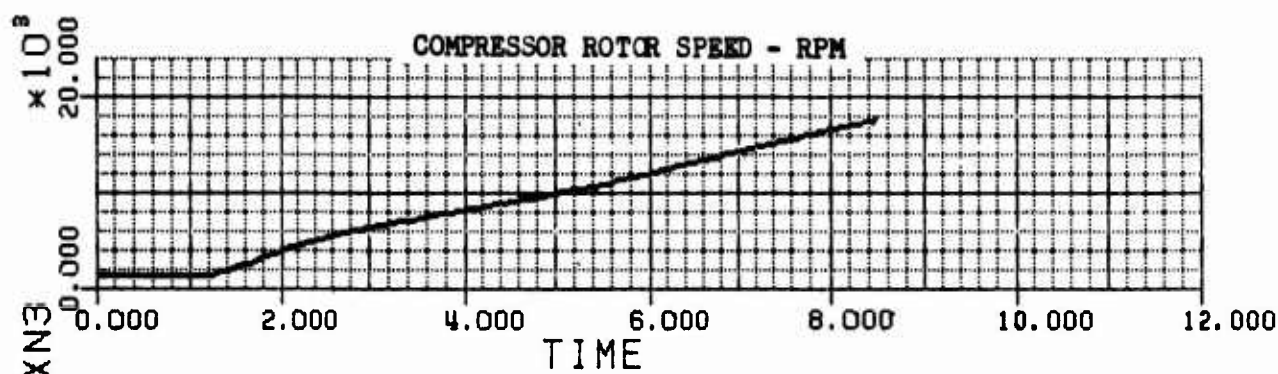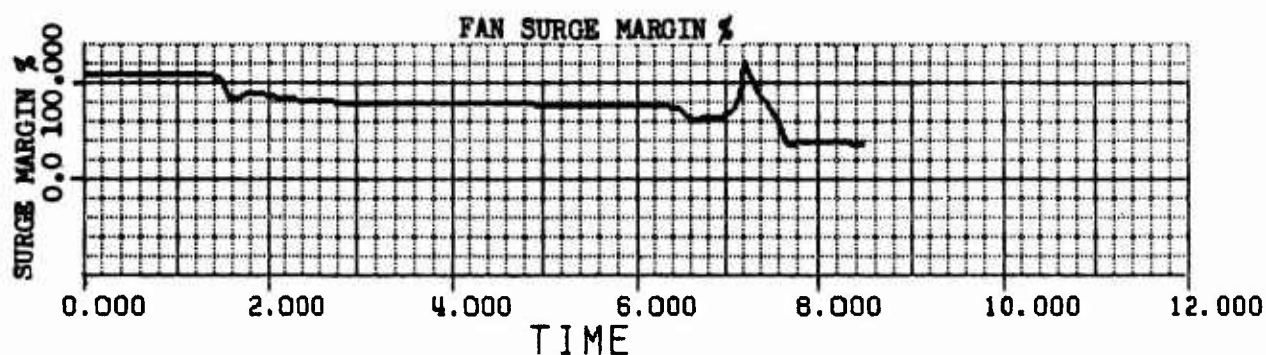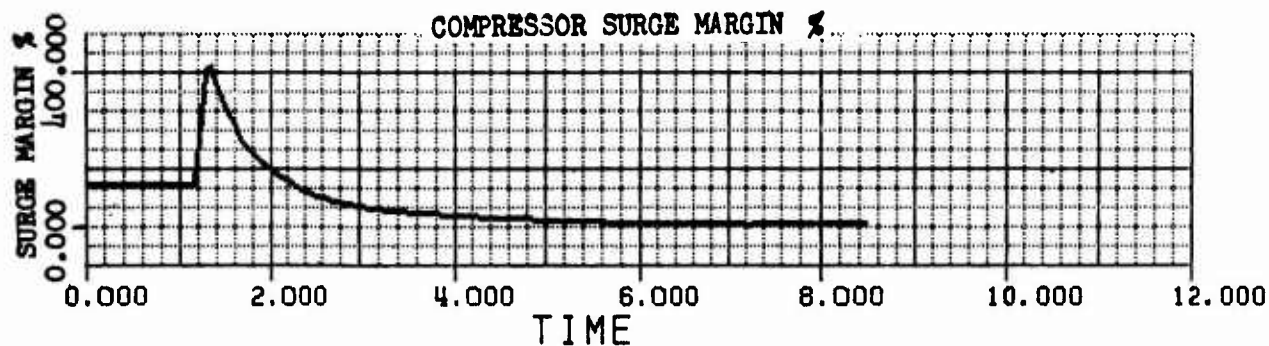to Turbofan (Continued)

SECTION IX

CONCLUSIONS AND RECOMMENDATIONS

A.   CONCLUSIONS

It is concluded that:

1.   The new concept of a combined fan duct/ram duct embodied in the P&WA STFRJ368 engine is a feasible design.

2.   The aerodynamic design of the fan/ram duct configuration performed under this program provides a stable, low-loss transition from the fan discharge to the common combustion chamber.

3.   The 1/8-scale model of the fan/ram duct configuration, including a rotating fan model, designed under this program, will provide the data needed to fully describe the aerodynamics of the fan/ram duct, specifically the fan and ram duct shutoff door characteristics (figure 12) and the dump and mixing process from the burners to the combustion chamber (figure 8).

4.   The digital dynamic simulation of the engine has been formulated and checked out as illustrated by the transient transition test cases.   However, these test cases do not represent designed or optimized transitions; they only demonstrate that the computer program is operational and ready for use in control mode studies in Phase II.

5.   Based on the effort under Phase I, transitions from turbofan to ramjet, and vice-versa, appear to be possible without unexpected problems; however, the planned Phase II effort is required to define and optimize the transition and to minimize perturbations.

B.   RECOMMENDATIONS

It is recommended that:

1.   The 1/8-scale fan/ram duct test rig designed under this program be fabricated and tested in order to provide the data needed to fully describe the aerodynamics of the fan/ram duct.

2.   The engine dynamic simulation developed and checked out under this program be used as planned in Phase II for control mode studies to define the control system required for a smooth, stable transition.

DOCUMENT CONTROL DATA - R & D

(Security classification of title, body of abstract and indexing annotation must be entered when the overall report is classified)

1 ORIGINATING ACTIVITY (Corporate author)	2a. REPORT SECURITY CLASSIFICATION
Pratt & Whitney Aircraft Division of United Aircraft Corporation Florida Research and Development Center	Unclassified
	2b. GROUP

3 REPORT TITLE

Fan/Ram Duct Program.
Phase I Final Report

4. DESCRIPTIVE NOTES (Type of report and inclusive dates)

Final Report, October 1972 – October 1973 on Phase 1,

5. AUTHOR(S) (First name, middle initial, last name)

Daniel E. Booz, Jr., Al Levesque, Edward B. Thayer

6. REPORT DATE	7a. TOTAL NO. OF PAGES	7b. NO. OF REFS
October 1973	56	None

8a. CONTRACT OR GRANT NO.	9a. ORIGINATOR'S REPORT NUMBER(S)
N00140-73-C-0003	PWA – FR-5936
b. PROJECT NO.	
c. 6φp.	9b. OTHER REPORT NO(S) (Any other numbers that may be assigned this report)
d.	N/A

10. DISTRIBUTION STATEMENT

Distribution of this report is controlled and each transmittal outside the department of defense requires prior approval of the Commanding Officer, NAPTC, Department of the Navy, Trenton, N. J., 08628

11. SUPPLEMENTARY NOTES	12. SPONSORING MILITARY ACTIVITY
N/A	Naval Air Propulsion Test Center Trenton, N. J., 08628

13. ABSTRACT

(trade mark)

The Phase I program described in this report is the initial 12-month effort of a planned three-phase program. It started with an analysis of the aerodynamics of the combination fan duct/ram duct used in the P&WA™ STFRJ368 turbofan-ramjet study engine. This was followed by the design of an aerodynamic test rig simulating the fan/ram duct configuration, including a model fan. The rig will be tested in Phase II to provide aerodynamic data (loss coefficients, flow profiles, etc.) at various steady-state points during the transition from turbofan to ramjet.

A digital dynamic engine simulation computer program was also formulated and checked out during Phase I. The checkout of the program was carried through transient transition test cases to validate the simulation. However, the test cases are not designed or optimized transitions; they illustrate that the computer program is operational. The computer program will then be used for transition control studies in later phases to define the control system and logic required for engine operation and smooth, stable transition from turbofan to ramjet and vice-versa.

DD FORM 1473 1 NOV 65

401355

14 KEY WORDS	LINK A		LINK B		LINK C	
	ROLE	WT	ROLE	WT	ROLE	WT
Turbofan-Ramjet Engines						
High-Mach Engines						
Dynamic Simulation						
Aerodynamics						